



## CHAPTER IV

### RESULTS AND DISCUSSION OF POLYPYRROLE-COATED LATEX PARTICLES BY ADMICELLAR POLYMERIZATION

#### 4.1 Abstract

The conducting composites were prepared by an electrochemical method using a pyrrole monomer in natural rubber latex. Polypyrrole (PPy) is a good electrically conductive polymer; however, it has poor processibility and its flexibility is limited. To overcome these limitations, electrochemical and admicellar polymerization with sodium dodecyl sulfate (SDS) is used. The admicellar polymerization of PPy by an electrochemical method over natural rubber particles was investigated by varying monomer content and applied voltages. The success of synthesis was confirmed by FTIR, SEM and TEM. Moreover, the TGA curves of the admicelled products revealed the shift to higher decomposition temperature than that of pure PPy. The mechanical property of the admicelled PPy/NR was also developed to be stiffer than that of natural rubber. The conductivity of the modified rubber is about  $10^{-9}$  to  $10^{-4}$  S/cm, which is much higher than that of natural rubber by several orders. Conductive rubbers can be used instead of the metallic conductors because the soft materials have the obvious advantage of flexibility and the ability to absorb mechanical shock.

#### 4.2 Introduction

Rubbers are usually electrically insulation used today. Although conductive rubber has been known since the latter part of the nineteenth century, it was not of major interest until about 1930. Rubber can be rendered conductive by the incorporation of an adequate loading of carbon black, as low as 20 parts per 100 parts (by weight) of the raw rubber. The particles of carbon black range in diameter from 10 to 300 millimicrons and are formed by burning or cracking hydrocarbon oil or gases. These particles tend to form themselves into chains, instead of being randomly dis-

persed, and the carbon chains give rise to the conductivity of the rubbers. The values of resistivity which may attend lie between 1 ohm.cm and  $10^{15}$  ohm.cm (Norman, 1970)<sup>1</sup>.

Conductive rubber could be used instead of the metallic conductors because the soft materials have the obvious advantage of flexibility and the ability to absorb mechanical shock. Both soft and rigid materials have the following advantages over metals (Tasakorn, P.1999)<sup>2</sup>:

- (i) Ease of shaping, flexible
- (ii) Low density, lightweight
- (iii) Wide range of electrical conductivity
- (iv) Low thermal conductivity
- (v) Corrosion resistance

Currently, many works are devoted to the synthesis of conducting polymers for use in a variety of applications, mainly for electronic and optical devices as well as for various industrial applications, eg. as semi-conductive textiles, including yarns and fabrics, and in military applications i.e. in radar-absorbing materials, camouflage netting, microwave antennas etc. Moreover, composites of electrically conductive particles in a non-conducting polymer matrix are materials with increasing importance as resistors in microelectronic devices, electrochemical devices, optical switching devices mechanical actuators and display devices, batteries, molecular electronics, nonlinear optics, electrical magnetic shields, microwave-absorbants, polymer light emitting-diodes (PLED), heating elements, electrically conductive adhesive, film and foams, or plastics dissipating static charges, and so on. (Gordon, G. 2003)<sup>3,13</sup>

Several attempts have been made to improve the processibility of conducting polymer through molecular design, copolymerization, and functionalized organic dopants. Usually, blending the nonconductive polymer with conductive polymers is a common and simple route to improve the processability and mechanical properties of conducting polymers, though this approach often results in a lowering of conductivity, and it is not easy to control the compatibility between two polymers and maintain the percentage of the conducting polymer. In this technique, insulating polymer.

rubber, has been combined with a number of conducting polymers such as polyaniline (PANI), polypyrrole (PPy), and polythiophene (PTH) in an aqueous or organic medium to produce conducting polymer composites<sup>4</sup>.

Polypyrrole is one of the most studied conductive polymers because of its good electrical conductivity, good environmental stability, biocompatibility, and relative ease of synthesis. Polypyrrole exhibits a wide range of surface conductivities ( $10^{-3} \text{ Scm}^{-1} < \sigma < 100 \text{ Scm}^{-1}$ ) depending on the functionality and substitution pattern of the monomer and the nature of the counter ion or dopant (Nalwa,1997)<sup>8</sup>. PPy can be prepared by electrochemical or chemical oxidation of pyrrole in various organic solvents and in aqueous media. Chemical polymerization is one of the best methods to prepare a large quantity (Bunsomsit,2002)<sup>9</sup>. However, the flexibility of PPy is limited by the nature of oxidizing reagents used and the reaction conditions employed. The limitations of PPy such as poor mechanical properties (e.g. brittleness and poor processability) have to be addressed in order to achieve satisfactory utility.

An organic dopant is one of the most important factors that can affect the properties of the conducting polymers. It has been demonstrated that one-step electrochemical polymerization of conducting polymer in the solubilized polyelectrolyte is an extremely convenient preparation technique (Pongprayoon,2002)<sup>10</sup>. Electrochemically polymerized PPy deposited on the electrode surface has been reported; the morphology and structure can be altered by the use of polymeric anions (Tasakorn,1996)<sup>11</sup>.

Recently, Chantarak. S. (2006)<sup>12</sup> reported the success of material polypyrrole (PPy) coated on the surface of natural rubber particles by admicellar polymerization using the Dodecyl Sulfate Sodium salt (SDS) as surfactant at various pyrrole concentrations.

The main objective of this study is to investigate the possibility of using electrically synthesized conductive polymers into a natural rubber structure as admicelled polymerization. In this study, natural rubber particles as the substrate were coated by admicellar polymerization of the polythiophene with SDS as the surfactant.

This research focuses on the influences of pyrrole content and thiophene content, pH, time, and voltage on the morphology. Furthermore, it also studies the mechanical properties. thermal properties, and conductivity were investigated.

## 4.3 Experimental

### 4.3.1 Materials

In this research, the natural rubber latex used as the substrate for electrochemical polymerization was provided by Rubber Research Institute, ~60% DRC. The anionic surfactant, selected for this experiment was Sodium Dodecyl Sulfate (SDS). A schematic of the chemical structure of SDS is shown in Figure 3.1. SDS was purchased from Aldrich Chemical Company, Ltd. with 99% purity<sup>[89]</sup>. According to Rosen (1996) the CMC of SDS was determined to be  $\sim 1.58 \times 10^{-3} \text{ mol/dm}^3$  at 25 °C. Hydrochloric acid used as doping and adjust PH. The pyrrole monomer (Aldrich) was first purified by distillation at 131°C and stored and refrigerated at 4°C before using in polymerization. Pyrrole monomer: purum 97% GC, Mr =67.06, bp =120-131 °C,  $d_4^{20}$ =0.970.

### 4.3.2 Equipments

The instruments and ASTMs are shown in Table 4.1 and 4.2. respectively.

**Table 4.1** Parameters to be measured for admicelled rubber properties

Parameters	Instrument / Technique
Prepared and purified natural rubber	-Hot plate and magnetic stirrer -Centrifugator, Hermle Z383K (at 10000 rpm/20 min) (ASTM 1076-02)
Particle Size	-Particle Size Analyzer (Mastersizer X Ver 2.15) (45 mm lens, active beam length 2.4 mm)
Thermal properties and amount of polymer formed	Thermogravimetric Analyzer (Perkin Elmer, Pyris Diamond) Thailand co.,ltd
Surface morphology	Scanning electron microscope (SEM) (JEOL JSM-5200) with magnification range between 1000-5000 times using voltage 15 kv
Atomic morphology	Transmission electron microscope (TEM) (JEOL JEM-

	2100)
Tensile testing	-Lloyd LRX Universal Testing Machine (ASTM D882-91) -Instron Universal Testing Machine under (ASTM638M-91a)
Functional group	Fourier Transform Infrared Spectroscope (FTIR) (Nexus 670, HATR flat plate system with 45°C ZnSe crystal) PERKIN ELMER 1760X.
Surface and volume conductivity	Resistivity Test Fixture (Keithley Model 8009) and Electrometer/High Resistance Meter (Keithley 6517A). (ASTM D257-99)
Density	Sartorius approach, model :YDK01

**Table 4.2** Rubber compound test method

Property	method	Instrument
Tensile properties (Max stress, MPa Elongation to break, % modulus, MPa)	ASTM 638M-91a ASTM D882-91	Instron Model 1011 Lloyd Instruments LS 500
Hardness, Shore A and Shore D	ASTM D2240	Lever Loader Model 716
Tear strength	ASTM D2262-83	Lloyd Instruments LS 500

#### 4.3.3 Purification of the Natural Rubber Latex

The rubber latex has a 60%wt dried solid content. Rubber latex (4-8 g) was mixed with 50 ml distilled water and centrifuged two times at 20°C, 10000 rpm for 20 minutes to removed dissolved impurities. Then, particles were resuspended in water and adjust pH <3.0 by using HCl.

#### 4.3.4 Particle Size Measurement

The particle size of natural rubber was determined by a particle size analyzer, Masterizer X version 2.15 (Malvern Instruments Ltd.). The lens used in this experiment was 45 mm for particle size 0.1-80 µm and active beam length was set at 24 nm. The sample was placed in a sample cell across a laser beam. This machine analyzed the average particle size and standard size distribution from the laser beam de-

pending on the beam length parameter. Consequently, the specific surface area was calculated from the particle diameter with the assumption of constant volume of a spherical particle.

A droplet of surfactant was added in a stirring water chamber in order to aid the distribution of natural rubber in water. After that, 0.03 vol% of natural rubber aqueous solution was suspended in a stirring water chamber.

#### 4.3.5 Polymerization of Pyrrole onto Latex Particle

##### **A.) Prepared Admicellar Polymerization of Pyrrole onto Latex Particles**

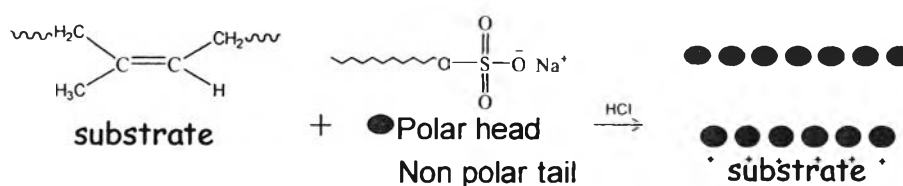
Concentrated natural rubber latex (4-8 g) was mixed with 50 ml distilled water and centrifuged two times at 20°C, 10000 rpm for 20 minutes. The 25 g of cream was separated and added in 10 ml distilled water. Then the rubber latex was mixed with surfactant solution, SDS, 16 mM, and make up volume to 500 ml (including amount of Pyrrole at various concentration 20-800 mM, 0.79-31.66 ml) by distilled water. HCl was added to maintain the pH of the solution at 3.0, which is the pH below the point of zero charge [11]. Then, it is stirred four hours to let the surfactant molecules form the bilayer at the surface of the rubber particles (Figure 4.1a).

The pyrrole solution (20–800 mM, 0.79–27.66 ml) was added and left for 1 hour (Figure 4.1b). Next, the apparatus for electrolysis was set up, and the aqueous solution was poured into the reaction bottle. Then, an additional current was passed through the solution containing the pyrrole monomer at various voltages and the solution was purge with N<sub>2</sub> to prevent the oxidation in the system (Figure 4.1c). As the current was applied across the cell, pyrrole was polymerized in the rubber latex solution at the cathode. The rubber was also pulled to cathode during polymerization and finally conductive natural rubber occurred on the cathode, (the copper has a dimension of 3.5x7 cm), as shown in Figure 4.2.

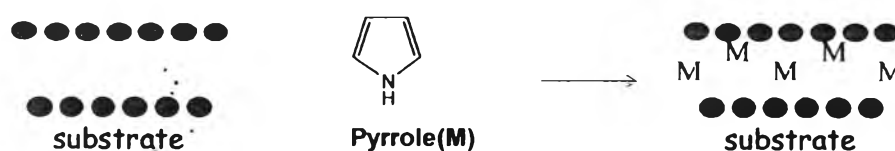
After the electro-polymerization has started, the pH and mass on the electrode are checked every hour and the electrode was replaced. The pH was adjusted to 3.0 by HCl. After the polymerization was complete, the dark solid rubber on the working electrode was washed with water to remove the surfactant, followed by drying in a vacuum oven at 70°C for 12 hours and black sheet with a constant weight was obtained. The solution changed from white to black and finally to clear solution (Figure

4.1d). In order to obtain the best synthesized conditions, factors such as applied potential (voltage), time, %yield and pH were studied. Mass can also be controlled by these factors. The voltage was applied by using an adaptor (0-30 Voltage, 3A, Kenji-model: K01). The average electrode sizes were about 3.5 x 7cm.

### a. Step 1. Admicelle Formation



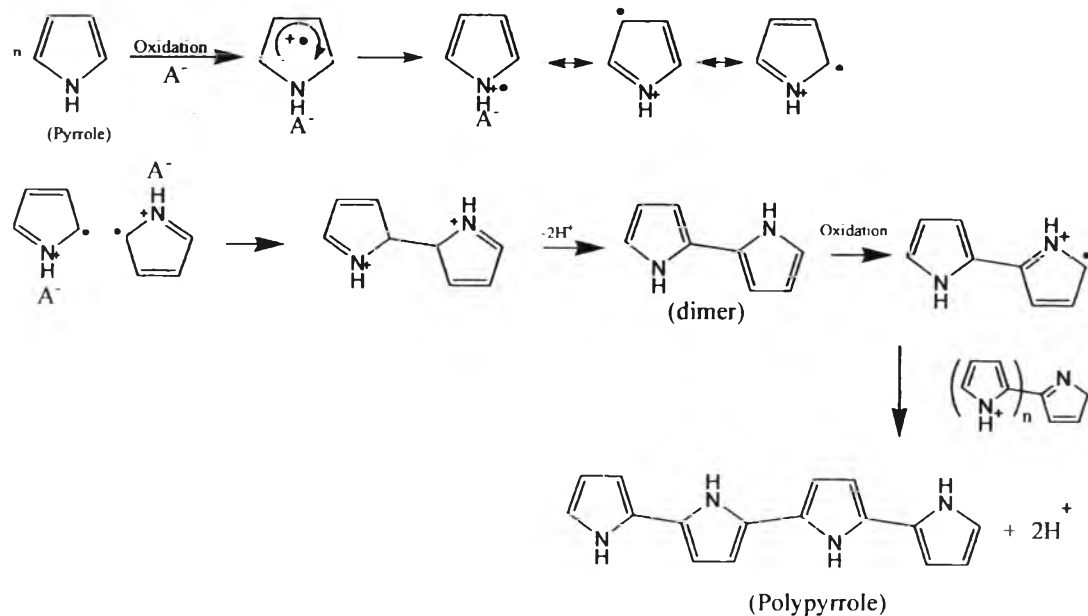
### b. Step 2. Monomer Adsolubilization



### c. Step 3. Polymer formation



#### Applied voltage



**d. Step 4. Surfactant Removal**

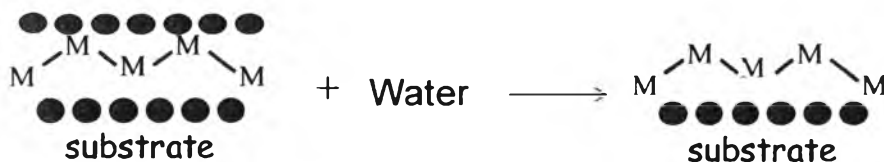


**Figure 4.1** Phenomena of admicelled polymerization.

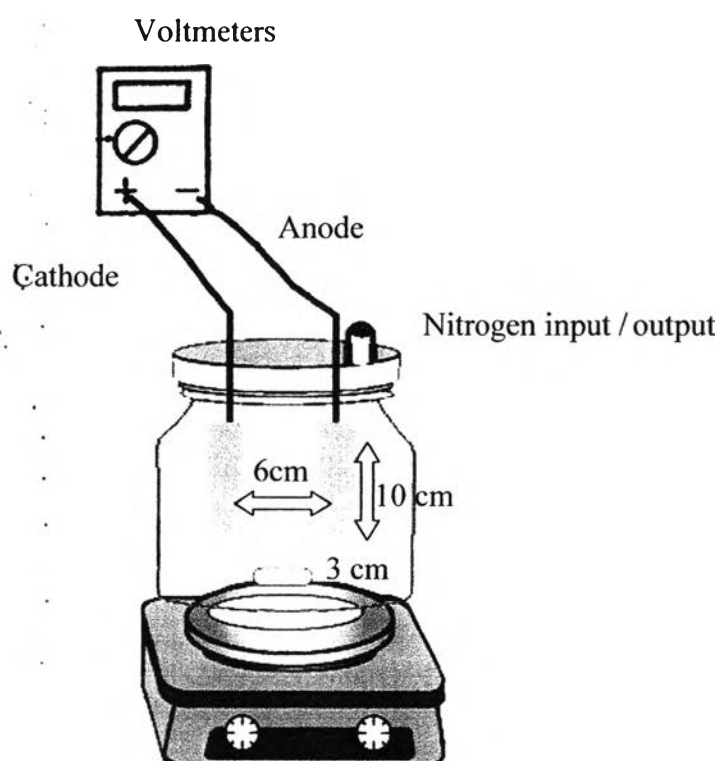


**Figure 4.2** Apparatus for admicelled polymerization with electrolysis. It consists of a reaction bottle and cover, cathode and anode electrodes, a voltmeter, an ammeter, a current supply, a hot plate and a magnetic stirrer.



#### 4.3.6 FT-IR Observation

The adsorption of the admicelled rubber films with a thickness of 0.3–0.8 mm obtained by compression at 160°C under a pressure of 25 tons for 15 min, were determined using the horizontal attenuated total reflection accessories for the FTIR (Nexus 670, HATR flat plate system with 45°C ZnSe crystal) to measure the spectra of materials. The spectra were recorded in the absorbance mode in a wavenumber range of 400–4000  $\text{cm}^{-1}$ . The sample spectra were recorded by using air as a background.

The KBr technique was used to prepare the powder sample of pure PPy for recording the spectrum. The specimen of pure PPy was prepared by grinding the powdered PPy with the KBr powder. The mixture was molded in special dies under a pressure of 10 tons. The sample spectrum was recorded by using KBr as a background.

#### 4.3.7 Determination density

The density of the specimens was measured using the Sartorius approach, model:YDK01, where the sample is weighed in air and then in water by a balance with a reproducibility better than 10  $\mu\text{g}$ . Each measurement represented the average of at least 3 specimens.

**Density of H<sub>2</sub>O**      0.9964      (from table at 25°C)  
**temperature**      27.5

$$\text{Eq} \quad d = \frac{w_a \times d_{\text{H}_2\text{O}}}{(w_a - w_{fl}) \times 0.99983} + 0.0012 \dots \text{g/cm}^3 \quad (1)$$

$$G = W(a) - W(fl) \quad (2)$$

Where:  $w_a$  = weight of solid in the air;  $w_{fl}$  = weight of solid in the liquid;

$G$  = buoyancy of the glass plummet;  $d$  = density

Pycnometer method is applicable to determinate the PPy particle density. This procedure is simple by using a know volume bottle, typically 25 ml. The measurement was done at 27.5°C.

$$\text{Solid sample of PPy} \quad \text{Sp.gr. } 27.5/27.5^\circ\text{C} = \frac{a \times d}{a + w - b} \quad (3)$$

where: a = mass of solid ; b = mass of pycnometer filled with water + solid at 23°C ;  
 e = mass of Pycnometer; d = sp.gr. 23/23°C of liquid;  
 w = mass of pycnometer filled with water

#### 4.3.8 Morphology study

There are two steps for studying the morphology. Firstly, the admicellar synthesized PPy on NR particles obtained from solution after polymerization was observed by a transmission electron microscope (TEM, JEOL, 2100). The magnification range was about 3000 -50 K.

Secondly, the morphology of the samples after polymerization and drying at 100°C for 6 hours was studied by SEM. The samples were taken into liquid nitrogen and then broken immediately to get cross section surface, and adhered to brass stubs. Next, the samples on the stubs were sputtered with a thin layer of gold. The morphologies of the admicelled PPy/NR were observed by a scanning electron microscope (SEM, JOEL model JSM-5200). SEM digitized photographs were obtained with a magnification range between 1,500–5,000 times using an acceleration voltage of 15 kV.

#### 4.3.9 Thermal properties measurement.

Thermal stability, moisture content, and decomposition temperature of the admicelled PPy/NR were studied by a thermogravimetric-differential thermal analyzer (Perkin Elmer, Pyris Diamond, TG-DTA). The samples were weighed at 10-18 mg and put in a platinum pan. The instrument was set to operate at temperatures from 30 to 600°C at a heating rate of 10°C/min under nitrogen atmosphere, 100 ml/min.

#### 4.3.10 Mechanical Properties Measurement

The mechanical properties for two specimen types were determined with one type (film shape) having a dimension of 20x100 mm (thickness 0.3-0.8 mm) as shown in Figure 4.3 Lloyd (UTM). The test was prepared by compression molding. The test followed ASTM D822-91 with a crosshead speed of 50 mm/min, a gauge length of 50 mm, and load cell 500 N under room temperature using Lloyd Universal Testing Machine. model :LRX. The test was repeated 5 times. The tensile strength

test uses two clamps to hold the testing strip. When secured, the testing strip is pulled apart. The yield point and breaking point is then measured.

The other specimen type is the dumbbell shape, which had a thickness larger than 3 mm. the specific sample size (Figure4.3) was cut by using a pneumatic punch following ASTM D638M-91a. The samples were tested by using the Instron Universal Testing machine with a crosshead speed 50 mm/min, a gauge length of 13 mm, and load cell 100 kN under room temperature. The test was repeated 5 times.

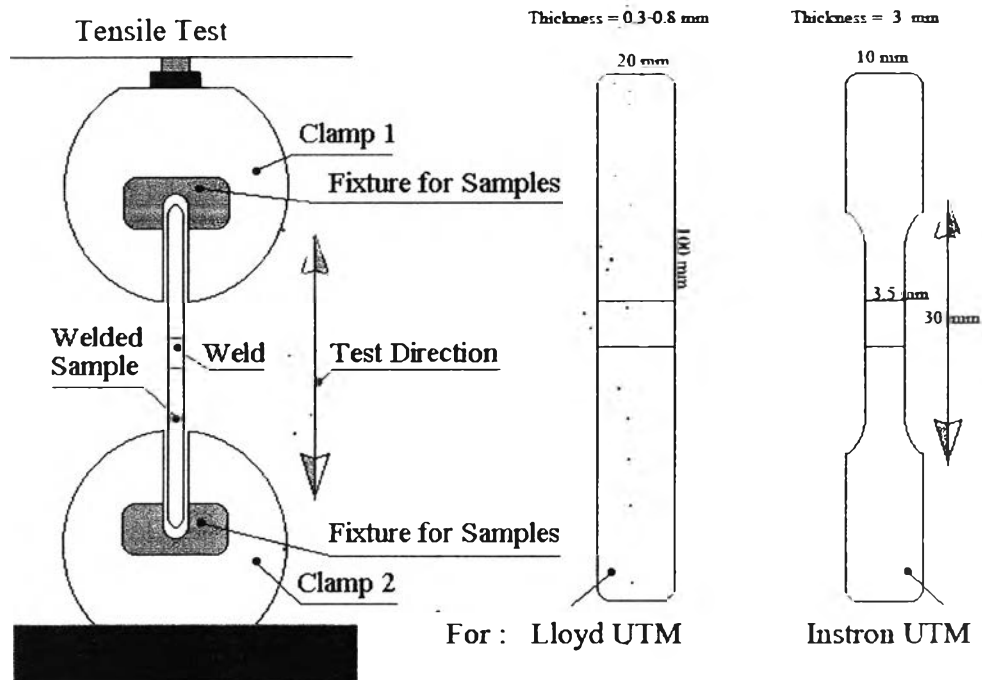


**Figure 4.3** Preparation samples for tensile test.

#### 4.3.11 Shore A and Shore D hardness Measurement

The flat specimen was placed on the plate. Then, the maximum height of the indenter was adjusted so that the tip of the indenter was approximately 10 mm above the test specimen. The unit was locked in position and the pointer was set to zero. The durometer probe was carefully, but fairly quickly and uniformly, lowered onto the test specimen. Then, initial shore hardness values were obtained by the pointer reading. According to ASTM D2240, the following conditions should be complied with :

- The test specimen should be at least 6 mm thick.

- The indenter should be at least 12 mm away from any edge of the specimen.
- At least 5 hardness readings should be taken per specimen.
- The instantaneous hardness reading on the dial gauge should be taken
- Only hardness values ranging between 10 and 90 are acceptable for shore A.
- If the value is greater than 90, the shore D test should be used instead.

#### 4.3.12 Conductivity Measurement

The admicelled rubber films from compression (thickness 0.3-0.8 mm) were cut into a round shape with six inches in diameter and tested for their surface and volume resistivity by using a Keithley 8009 Resistivity Test Fixture and a Keithley 6517A Electrometer/High Resistance Meter. A dc voltage from 0.1 to 15 volts was applied to the specimen placed in the Keithley 8009 test fixture. Then, the current was read and the surface and volume resistivity were determined (ASTM D-257).

The resistance,  $R$ , of the films was calculated using Eq. 4, the volume resistivity, surface resistivity and the conductivity were found using Eqs. 5, 6 and 7, respectively:

$$R = \frac{V}{I} \quad (4)$$

$$\rho_v = \frac{22.9V}{tI} \quad (5)$$

$$\rho_s = \frac{53.4V}{I} \quad (6)$$

$$\sigma = \frac{1}{\rho_v} \quad (7)$$

where  $R$  is the resistance (watts),  $V$  is the voltage (volts),  $I$  is the current (amperes),  $\rho_v$  is the volume resistivity (ohm centimeters),  $\rho_s$  is the surface resistivity (ohm),  $t$  is the film thickness (centimeters), and  $\sigma$  is the conductivity (siemens per centimeter).

## 4.4 Results and Discussion

### 4.4.1 Preparation of Natural rubber sheet.

Natural rubber latex consists of particles of rubber hydrocarbon and non-rubber constituents suspended in an aqueous phase. These natural rubber particles can be separated from the aqueous phase by centrifugal method. The natural rubber particle can be grown to the various thicknesses on the anode (a working electrode, size 3.5x7 cm). Effect of voltage applied across the cell on the natural rubber sheet is clearly shown in Table 4.3, Figures 4.4 and 4.5, and Appendix D respectively.

**Table 4.3** Effect of voltage on % yield and reaction times at pyrrole 100 mM(3.35g, 15.473%wt), NR latex(60%wt DRC) 25 g, and SDS 2.307g

<b>Voltage</b>	<b>6</b>	<b>9</b>	<b>12</b>	<b>15</b>
<b>%yield</b>	98%	94%	93%	129%
<b>Times for synthesis (hr)</b>	24	20	19	18

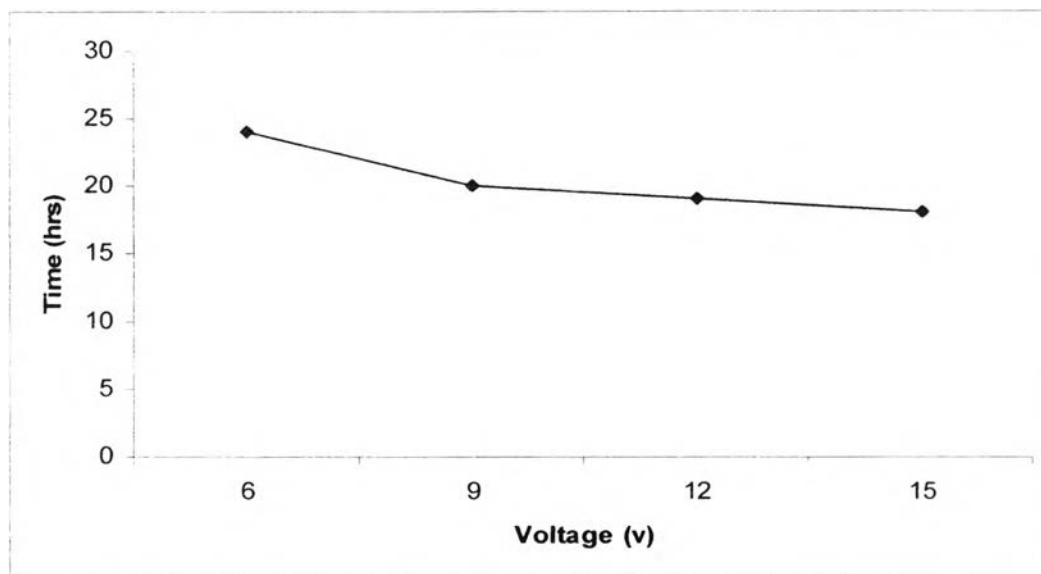


**Figure 4.4** Effect of voltage applied on reaction time.

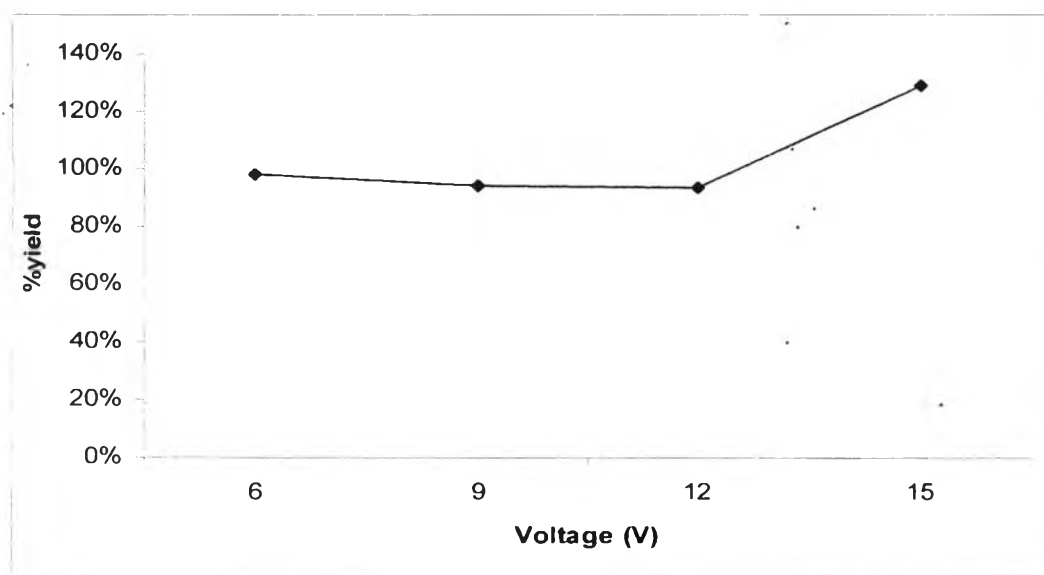


**Figure 4.5** Effect of voltage applied on % yield.

From Figure 4.4. the time to synthesize the admicelle rubbers, slowly decreased as the voltage increased. At higher voltage the increment of thickness and yield were not smooth. It can be postulated that high voltage induced the faster deposition of negatively charged rubber particles on the surface of the anode and the passivation or over-resistance occurred on the anode at the same time. At the highest voltage, 15V, the highest yield is shown because of the corrosion of copper, as shown in the Figure 4.5. However, voltages higher than 9 volts do not enhance the best deposition due to corrosion. Therefore, a voltage of 9 volt was chosen.

Next, the polymerization reaction was carried out for the admicellar polymerization of rubber with various pyrrole concentrations (20-800 mM) in the electrochemical method at 9V, 25°C. Table 4.4 shows the dependence of %yield and reaction times on the PPy concentration. It is also clearly shown in Figure 4.6 that %yield and reaction times of admicelled rubber were decreased along with the increased PPy concentration. The higher the concentration of PPy, the faster the reaction was (Tasakorn,1996)<sup>2</sup>.

**Table 4.4** Effect of PPy content on % yield and reaction times at 9 V, NR latex (60%DRC) 25g, and SDS 2.307 g

PPy	(mM)	20	50	100	200	500	800
	(g)	0.67	1.67	3.34	6.68	16.70	26.72
<b>Mass at anode (g)</b>		23.22	24.17	27.43	29.83	35.61	45.31
<b>%yield</b>		90.45	90.62	89.55	86.58	85.39	87.61
<b>Times (hr)</b>		35	32	20	15	13	10

When :  $\%yield = \frac{M_{total} \times 100}{(M_{NR} + M_{PPy})}$  ;  $M_{sds}$  is not calculated because it can be removed by water.

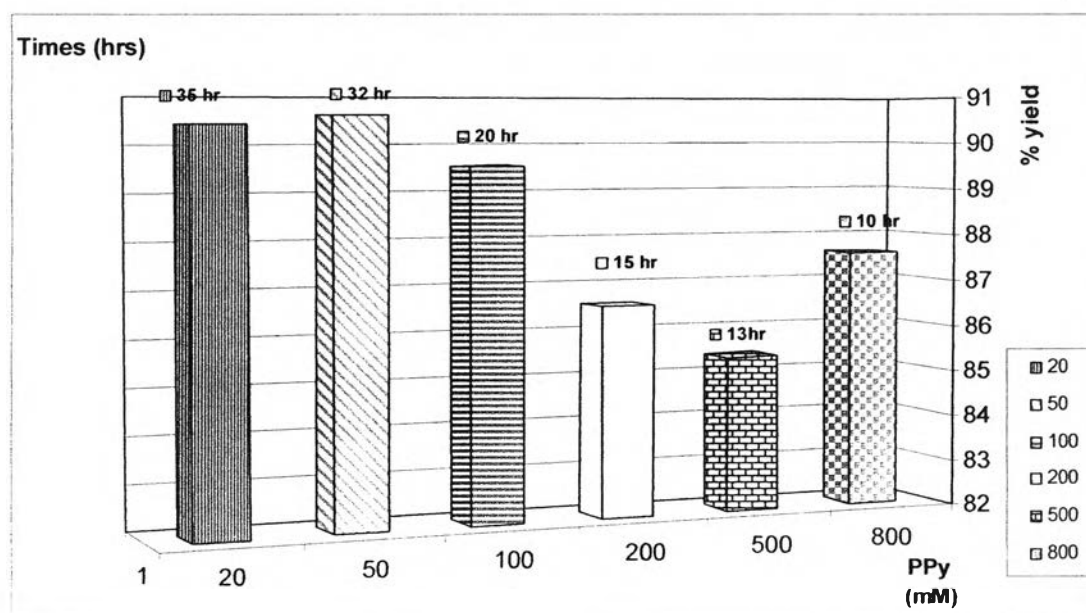


**Figure 4.6** Effect of pyrrole concentration on reaction times and %yield

Admicelled rubber was slowly deposited at the anode electrode as shown in Figure 4.7 and Appendix D. The success of polymerization can be determined the rate equation of accumulated mass at the anode electrode as below:

$$A2 : y= 6.88 \ln(x) +0.11 \quad (8)$$

$$A5 : y=7.58 \ln(x) -0.17 \quad (9)$$

$$A10 : y=9.29 \ln(x) -2.30 \quad (10)$$

$$A20 : y=11.25 \ln(x) -3.33 \quad (11)$$

$$A50 : y=15.01 \ln(x) -5.22 \quad (12)$$

$$A80 : y=20.01 \ln(x) -4.95 \quad (13)$$

Finally, the solution changed to a clear solution, indicating that the polymerization was completed. Then, other properties were observed

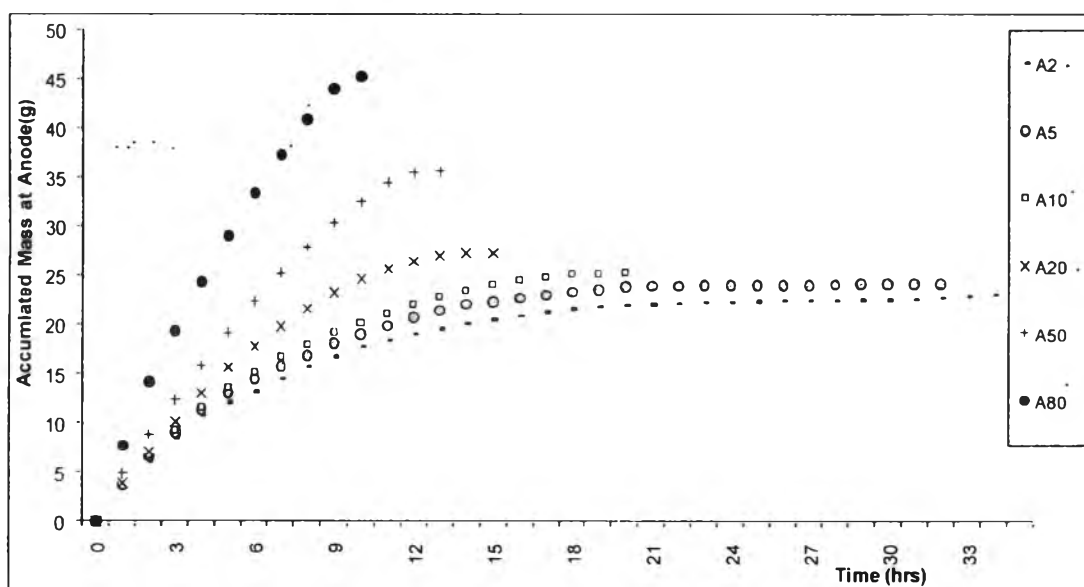


**Figure 4.7** Accumulate weight equation of admicelled rubber (PPy: NR).

Reaction conditions to induce high electrical conductivity of conductive natural rubber were studied in order to select the optimum conditions. The major parameters that influence the quality of conductive rubber prepared with various concentrations of PPy, 9V, 25°C is pH value. Bunsomsit, K et.al (2002)<sup>10</sup> studied the point of zero charge. The point of zero charge or net surface charge of zero is known from the intersection of the electrophoretic mobility curve and the zero axis. When the pH of the solution is equal to PZC, the surface charge of the substrate is equal to zero. At pH values below the PZC, the substrate surface exhibits a positive charge, then ani-



onic surfactants are adsorbed, or vice versa. In this study, the pH was adjusted to be less than 3.0 and the pH values were determined every hour until the clear solution obtained. The result is shown in Figure 4.8 and Appendix E (Table E1).

Effect of pH on reaction times is shown in Figure 4.8. It is apparent that the pH value increases with increasing reaction time. This is probably due to the preferred basic condition generated by the high conversion to PPy. This effect agrees with the reported by K.S. Jang (2004)<sup>156</sup>. Moreover, the correlation at low pH can be enhanced the conductivity due to severe protonation of the polymer backbone. On the other hand, the significant conductivity drop in the high pH range may be attributed to diminished effective  $\pi$ -conjugation length of the chain caused by repulsions between adjacent free sulfonate anions. The highly anionically charged polymer backbone under the strong basic conditions may also weaken the interactions with the dopants, thereby decreasing electrical conductivity<sup>156</sup>.

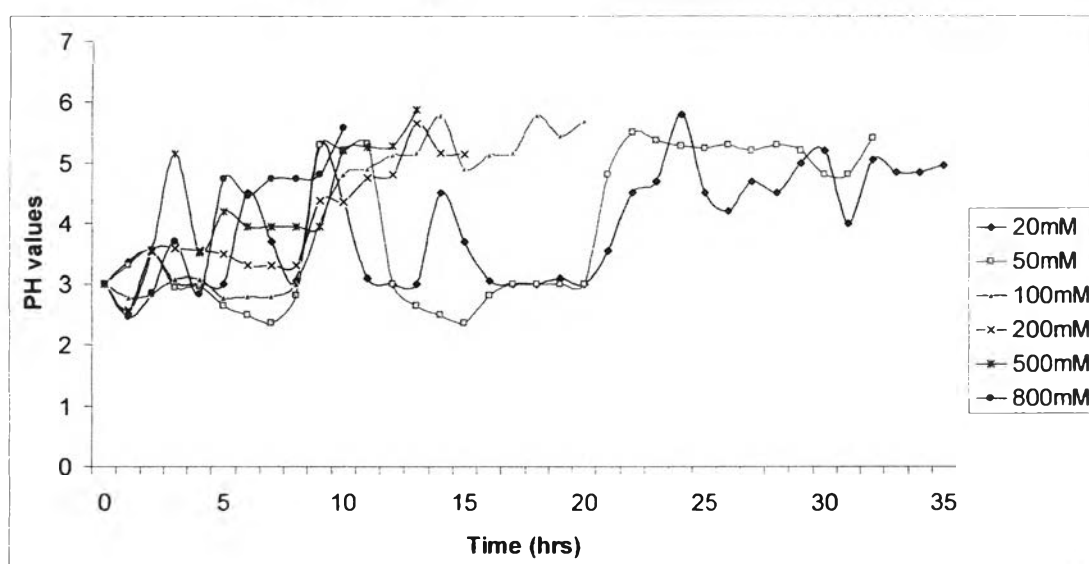


**Figure 4.8** Effect of reaction times on pH values.

#### 4.4.2 Fourier-Transform Infrared Spectroscopy of Admicelled NR Latex

The infrared spectra of pure rubber, pure PPy, and admicelled rubbers in the region from 4000 to 400  $\text{cm}^{-1}$  are shown in Figures 4.9– 4.12.

The obtained spectrum of pure polypyrrole (Figure 4.9) agrees with the IR spectrum reported by Vishnuvardhan T K., *et al.* (2005)<sup>103</sup>. The band at 1558 (2,5-substituted pyrrole) and 1457 and 1397  $\text{cm}^{-1}$  are assigned to typical polypyrrole ring vibrations. The bands at 1293, 1205, and 1119  $\text{cm}^{-1}$  can correspond to the =C-H band in the plane vibration. The broad band at 1178  $\text{cm}^{-1}$  is assigned to N-C stretching (Nicho and Hu, 2000)<sup>104</sup>. The IR peaks observed at 1030-657  $\text{cm}^{-1}$  are assigned to the =C-H out of plane vibration indicated polymerization of pyrrole (Scienza, 2003)<sup>105</sup>. IR spectrums of PPy are summarized in Table 4.5.

The obtained spectrum of pure rubber (Figure 4.10) confirms with the IR spectrum reported by Rippel M., *et al.* (2003)<sup>10</sup>. The band at 3036  $\text{cm}^{-1}$  corresponds to =C-H stretching. Bands at 2960, 2915, and 2853  $\text{cm}^{-1}$  are assigned to the C-H stretching of  $\text{CH}_3$ , the C-H stretching of  $\text{CH}_2$ , and C-H stretching of  $\text{CH}_2$  and  $\text{CH}_3$ , respectively. The principle peaks corresponding to isoprene functional groups of natural rubber are observed at 3036, 2960, 2915, 2853, 1662, 1448, 1375, 1129, and 834  $\text{cm}^{-1}$ . Several other peaks that are not associated with isoprene are also present: an intense broad band between 3200, 3500  $\text{cm}^{-1}$  indicating the presence of a hydroxyl group, and an amide (N-H) peak at 3280  $\text{cm}^{-1}$  (more apparent in cream rubber), a carbonyl (C=O) peak at 1737  $\text{cm}^{-1}$ , a small amide (N-H) peak at 1548  $\text{cm}^{-1}$  (both more apparent and more resolved in cream rubber), and a series of peaks between 1130 to 1010  $\text{cm}^{-1}$ , indicating oxygenated compounds. The peak at around 1080  $\text{cm}^{-1}$  is assigned to two categories: polyisoprene units and proteins/phospholipids (Rippel M., *et al.* 2003)<sup>106</sup>. IR spectrums of NR are summarized in Table 4.6.

The FT-IR spectra of all admicelled rubbers reveal the combined absorption of rubber and PPy. These results confirm the existence of PPy after polymerization in the rubber system. The absorbance of NR decreases as PPy content increases as shown in Figure 4.11-4.12 and IR spectrums are summarized in Table 4.7.

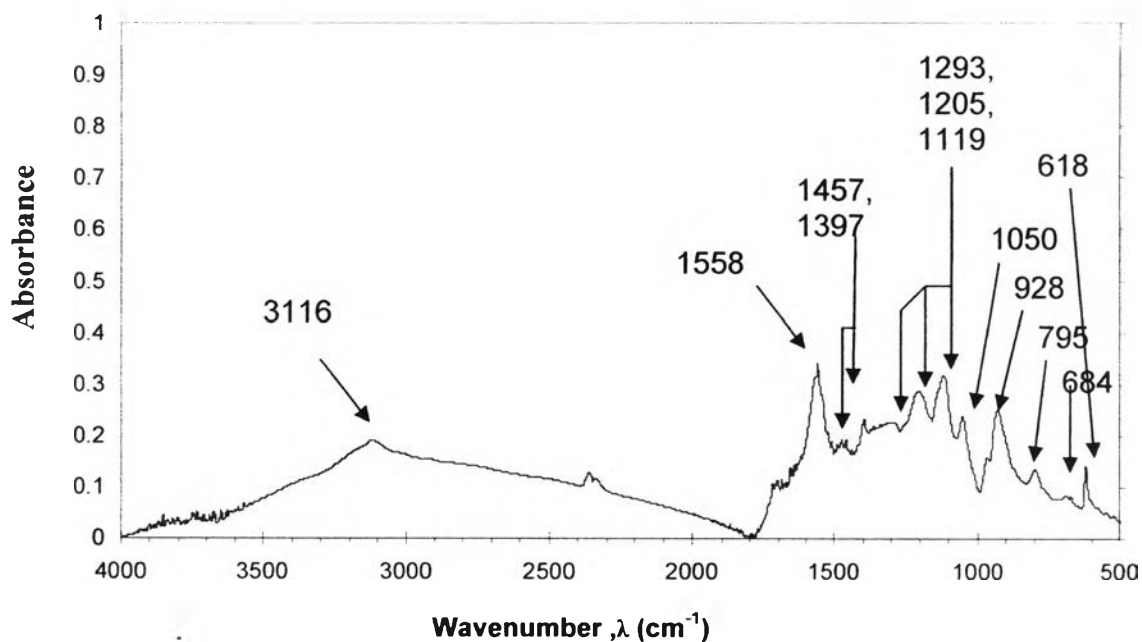


**Figure 4.9** FTIR spectrum of Polypyrrole

**Table 4.5** Assignment for the FTIR spectrum of pyrrole<sup>103,105</sup>

Wavenumber, λ (cm <sup>-1</sup> )	Assignment
3116	N-H stretching
1558	C=C stretching
1457, 1397	C-C stretching
1293, 1205, 1119	=C-H in plane
1050	N-H in plane
928	C-H stretching
795	=C-H out of plane
684	C-C out of plane
618	N-H out of plane

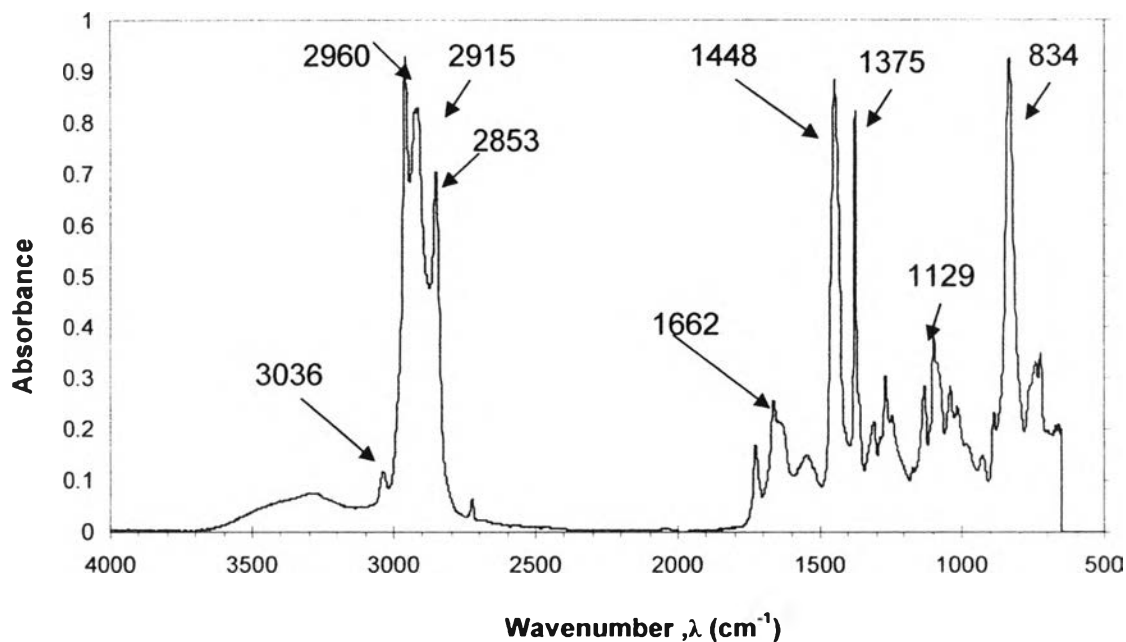


**Figure 4.10** FTIR spectrum of pure Natural rubber, Polyisoprene.

**Table 4.6** Assignment for the FTIR spectrum of isoprene<sup>106</sup>

Wavenumber, λ (cm <sup>-1</sup> )	Assignment
3036	=CH stretching
2960	C-H stretching of CH <sub>3</sub>
2915	C-H stretching of CH <sub>2</sub>
2853	C-H stretching of CH <sub>2</sub> and CH <sub>3</sub>
1662	C=C stretching
1448	C-H bending of CH <sub>2</sub>
1375	C-H bending of CH <sub>3</sub>
1129	C-H bending
834	C=CH wagging

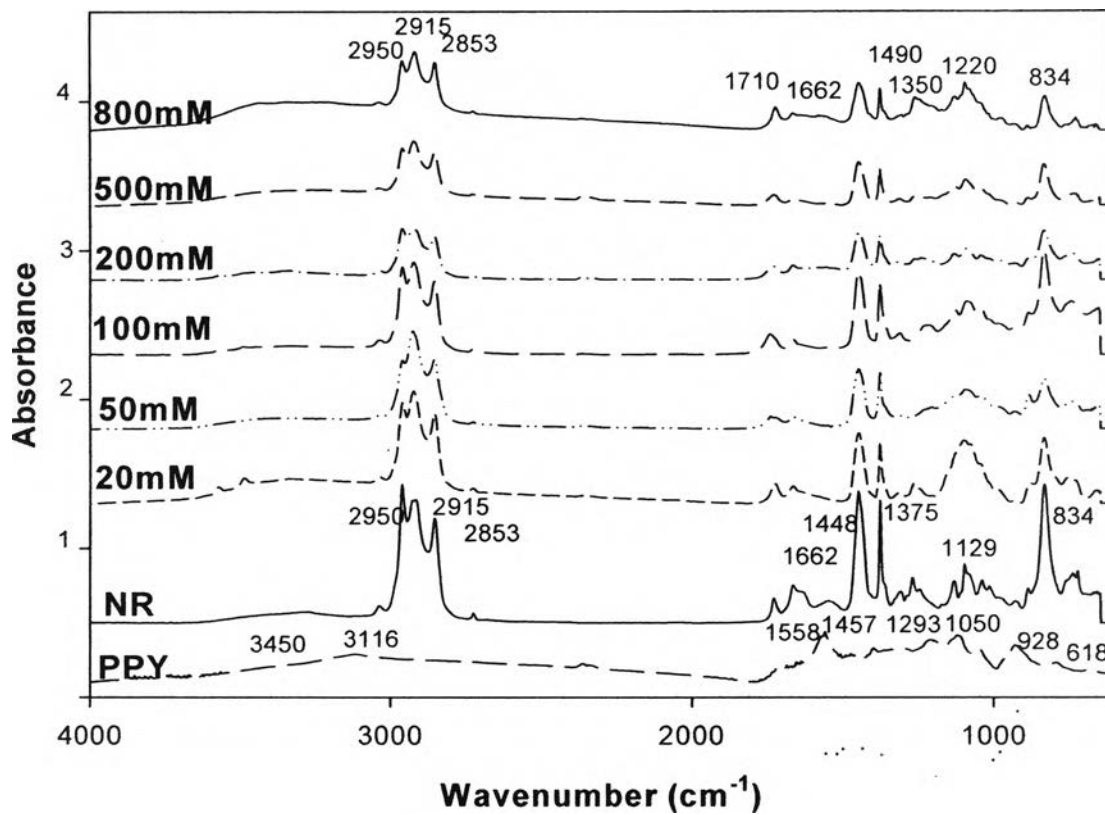


**Figure 4.11** FT-IR spectra of the admicelled rubbers with polypyrrole (HATR flat plate system with 45°C ZnSe crystal).

**Table 4.7** Assignment for the FTIR spectrum of combination<sup>103.104.105.106.107.108</sup>

Wavenumber, $\lambda$ (cm <sup>-1</sup> )	Assignment
3450,3116	NH stretching (PPy)
2950,2915,2853	CH stretching (NR)
1710,1558	C=C stretching (NR+PPy)
1662 ,1600	Ring stretching (PPy)
1490, 1350	CH in plane bending (NR)
1220, 1180, 1160, 1100	Doping- induced mode (PPy)
660, 620, 600	Aromatic ring (PPy) and CH out of plane (NR+PPy)

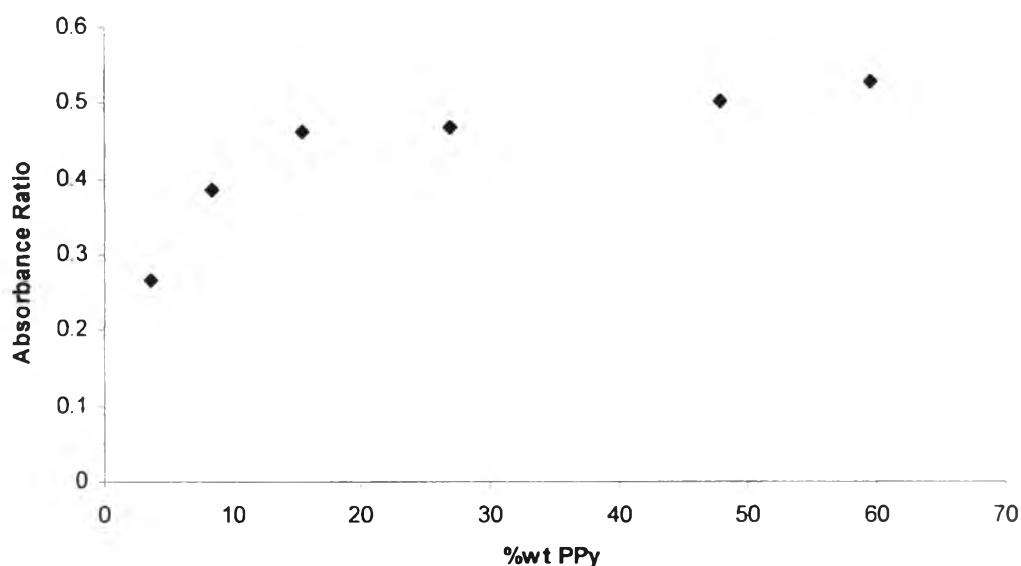


**Figure 4.12** The Absorbance ratio ( $1050\text{cm}^{-1}(\text{PPy})/2915\text{cm}^{-1}(\text{NR})$ ) at difference concentration.

#### 4.4.3 Density measurement

To further understand the change of properties in NR/PPy composites, an experiment was done to give more detail about the density. The density of specimens was measured using the Sartorius approach, model :YDK01, where the sample is weighed in air and then in water with a balance with a reproducibility of better than  $10\ \mu\text{g}$ . Each reported measurement represented the average of at least 3 specimens, which were calculated by using the following equation:

**Density of H<sub>2</sub>O**      0.9964      (from table at 25°C)  
**temperature**      27.5

$$\text{Eq } d = \frac{w_a \times d_{H_2O}}{(w_a - w_f) \times 0.99983} + 0.0012 \dots \text{g/cm}^3$$

$$G = W(a) - W(fl)$$

$w_a$  = weight of solid in the air

$w_a$  = weight of solid in the liquid

G = buoyancy of the glass plummet

d = density

Pycnometer method is applicable to determinate the PPy and PTh density. This procedure is simple by using a know volume bottle, typically 25 ml. The measurement has to carried out at a certain temperature by filling the liquid sample in the pyconometer bottle unit it is full and cap is put on. At this point the volume of liquid sample is equal to the bottle volume, i.e. 25 ml. Then the bottle is cleaned and weighed to a constant weight. Density is then calculated; divided measured weight by bottle volume. It shows more details in Appendix I and Table I-1.

The density of admicelled NR increases gradually with PPy content (Figure 4.13), the abrupt change in density is found at 800 mM PPy. In addition, the results show that the admicelled NR samples have densities lower than 1 (unity) and higher than that of NR but lower that of PPy and pyrrole monomer. This suggests the admicelled NR is light although the dense pack of PPy is observed. As observed in the Table 4.8, both of experimental and calculation of density are nearly same results. The increase in the density of PPy becomes form PPy tiny globules (at low amount of PPy) to reside, which explains the same reason by using TEM. The PPy tiny globules was also surrounded the NR particles and in the swollen region. This interesting to note that as PPy content increase ( $\geq 100\text{mM}$ ) the tiny globule packing becomes denser, as a result, the rough surface coating become smooth coating.

Thus, the admicelled rubber particles have more opportunity to contact each other. As the volume fraction of PPy increased to the critical value, the conductivity mechanism of PPy in the polymer changes from the tunneling effect to direct contact, and the conductivity of the polymer composites increase dramatically. These changes in conductivity are present in Appendix G and Section 4.4.10.

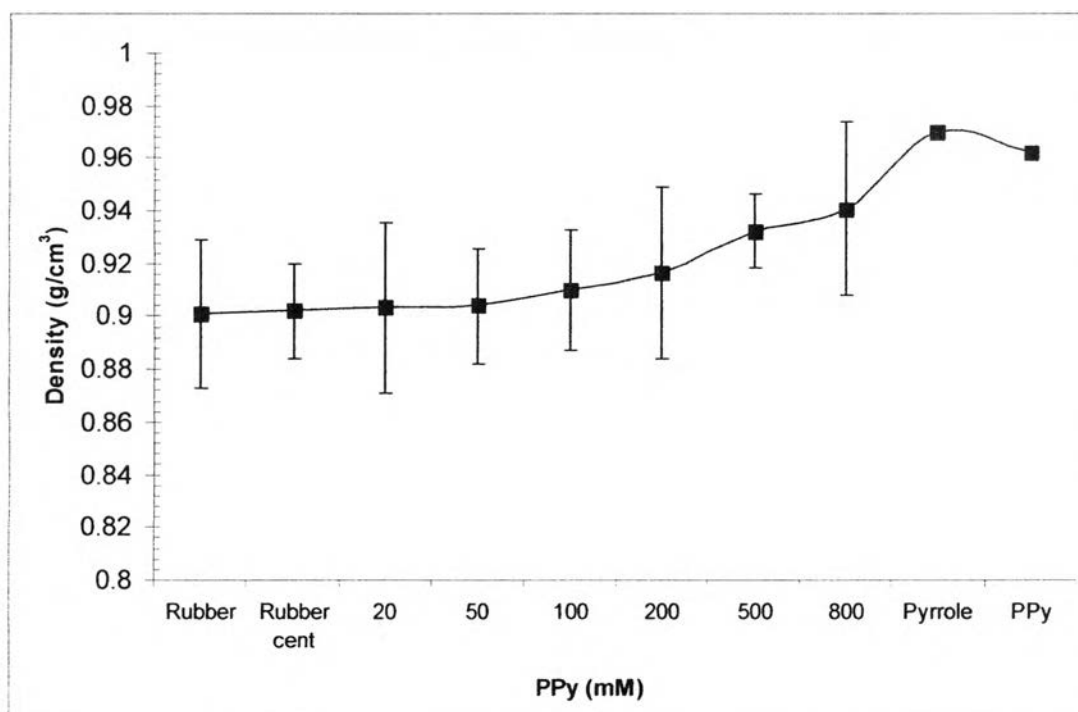
Thus, the higher number of polymer chains was obtained when content is high to abstract electron from pyrrole and enhance free radical polymerization, resulting in higher conductivity and higher in their density.

**Table 4.8** Measurement density of conductive polymer

Sample	w. air	w. fl	G	$d_{\text{experimental}}$	$D_{\text{calculation}}^{**}$	$d_{\text{calculated of PPy}}^{***}$
Rubber	0.28101	-0.0291	0.3112	$0.9011 \pm 0.028$	0.9011	-
Rubber (centrifuge)	0.28369	-0.0301	0.31379	$0.9022 \pm 0.018$	0.9022	-
20	0.28101	-0.0291	0.3112	$0.9033 \pm 0.032$	0.9045	0.9032
50	0.28369	-0.0301	0.31379	$0.9040 \pm 0.022$	0.9078	0.9181
100	0.23072	-0.02417	0.25489	$0.9101 \pm 0.023$	0.9126	0.9526
200	0.26982	-0.02802	0.29784	$0.9164 \pm 0.0326$	0.9203	0.9561
500	0.2169	-0.02092	0.23782	$0.9325 \pm 0.0142$	0.9346	0.9673
800	0.2213	-0.01966	0.24096	$0.9409 \pm 0.033$	0.9425	0.9689
Pyrrrole				0.9700	0.9700	-
PPy				0.9620*	0.9620*	-

\* Measurement the density of solid particle by using Pycnometer (in appendix I)

\*\*Calculation density from %wt and \*\*\*Calculation the density of PPy in specimens (in appendix J)

**Figure 4.13** Variation of density with polypyrrole concentration for admicellar rubber



#### 4.4.4 Particle Size Distribution of NR Latex

The particle size distribution of NR latex before admicellar polymerization showed a mean diameter of 1.05  $\mu\text{m}$  and a mean specific surface area of 6.874  $\text{m}^2/\text{g}$ . These results indicate the polydispersity of NR latex particles with narrow size distribution (Figure 4.14).

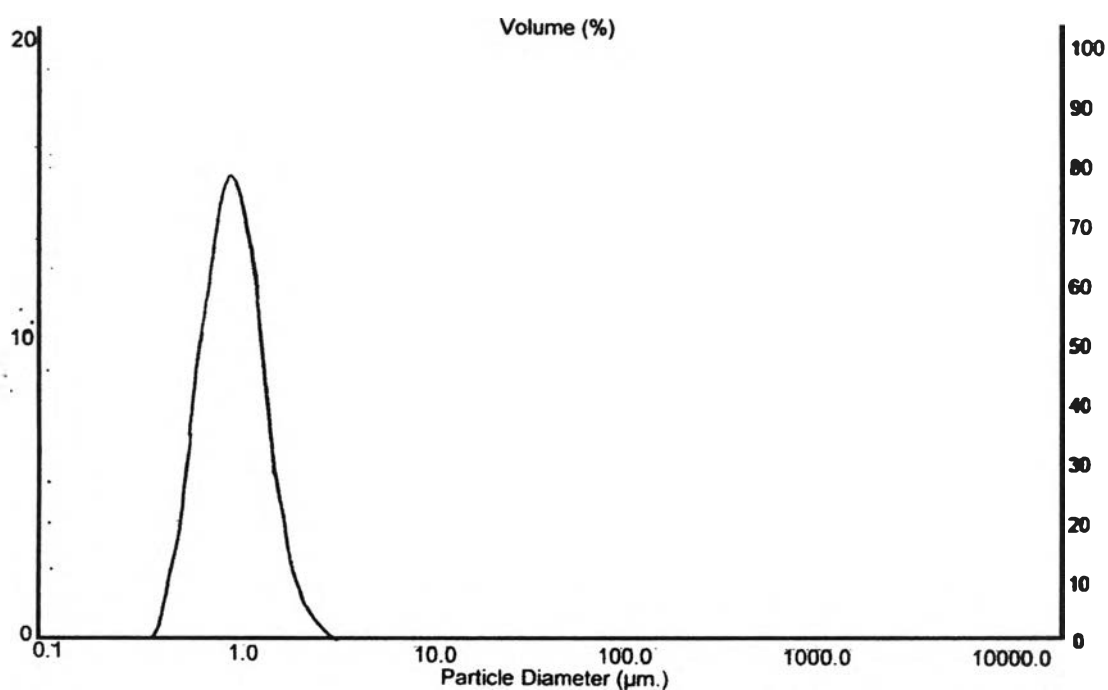


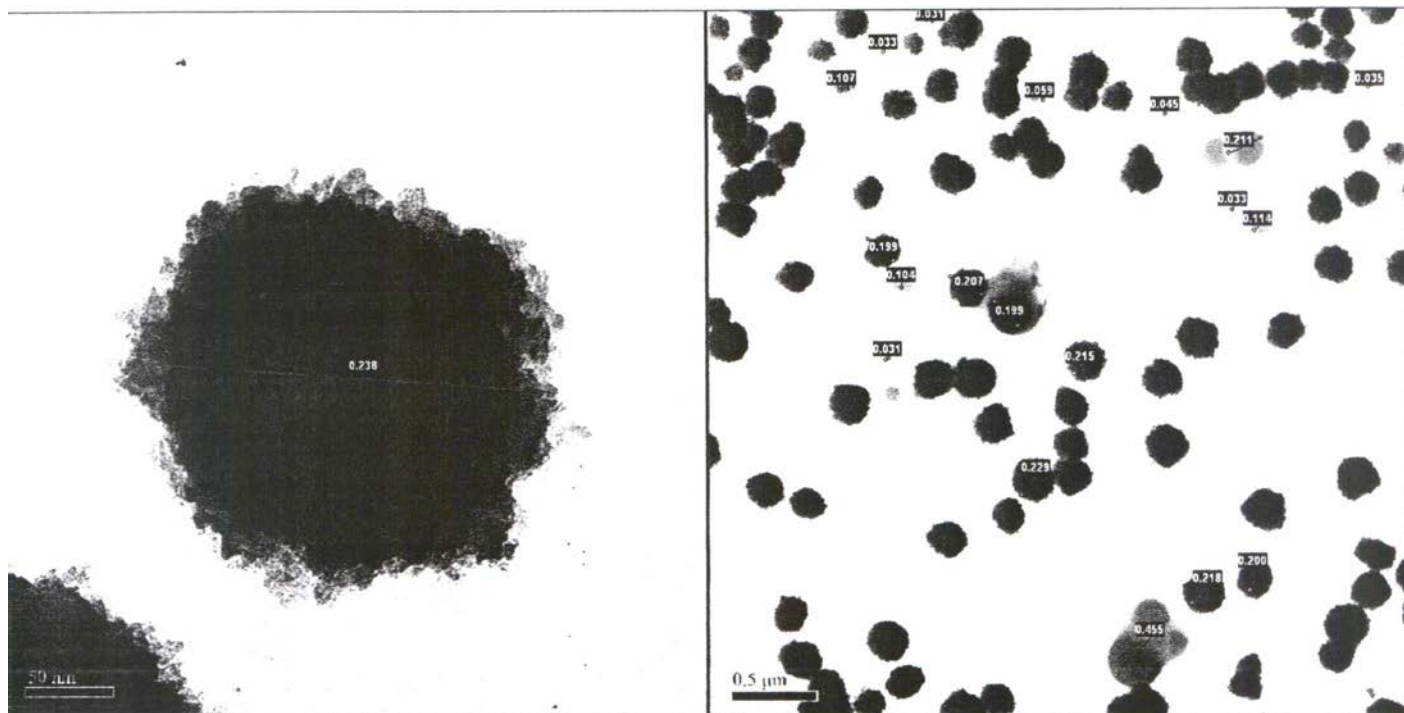
**Figure 4.14** Histogram showing the particle size distribution by volume of the natural rubber latex.

#### 4.4.5 Transmission Electron Microscopy (TEM)

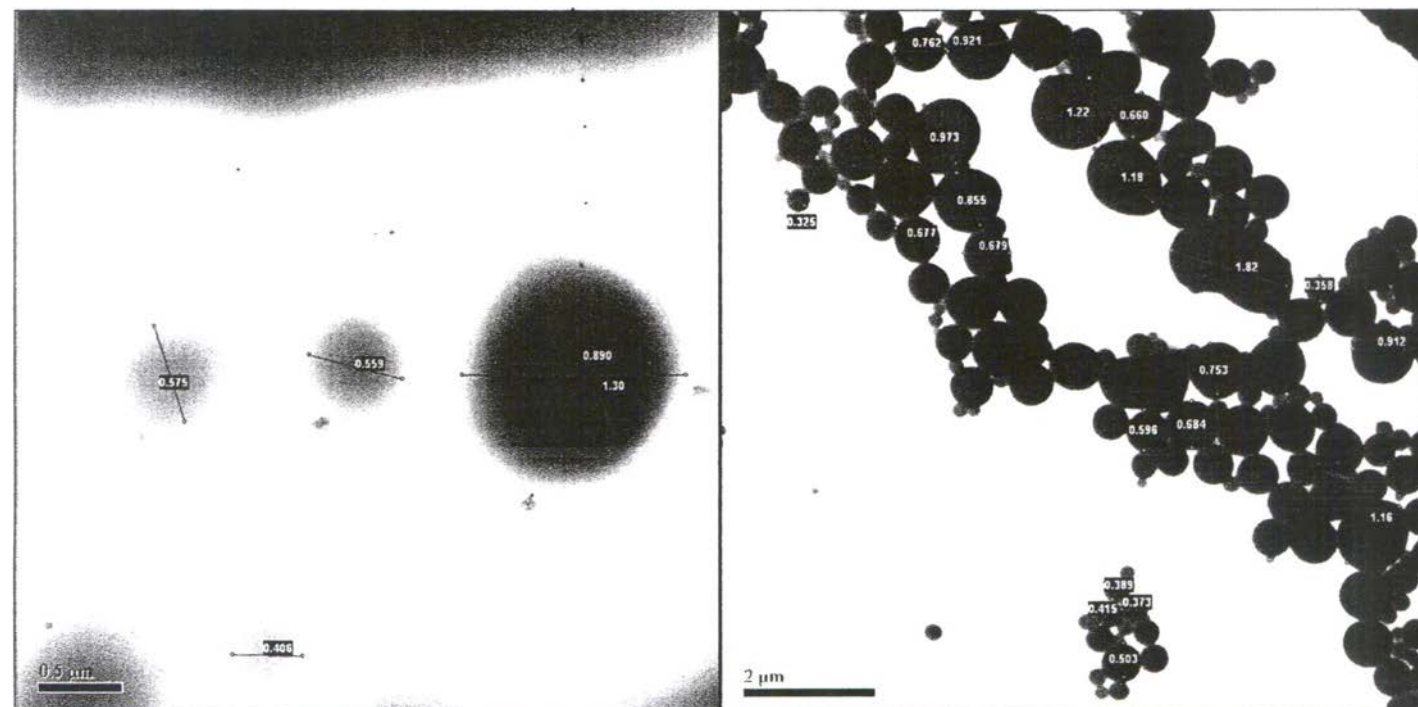
The morphologies of the admicelled rubbers were investigated by transmission electron microscopy (JEOL-JEM 2100) at 200 kV. The TEM micrographs and nanographs of the admicelled rubber with different PPy concentrations reveal the round shape of rubber particles with an evenly coating conductive polymer over the particles. The sample shows latex particles coated by SDS, and the PPy layer as a core-shell structure where the NR particle is the core and PPy is the shell. The samples, natural rubber, with 20, 50, 100, 200, 500, and 800 mM of polypyrrole clearly show coating of PPy on each latex particle individually, as shown in Figures 4.15-4.23. The average core particle diameter was estimated to be between 0.5 and 0.9  $\mu\text{m}$  and the coating particles were between 0.8 and 2  $\mu\text{m}$ .

Figure 4.15 shows the primary particles of pyrrole, size diameter about 20-30 nm. They form into globular aggregates with rough surface of 100-250 nm. Figure 4.16(left) shows NR particles with no OS staining, it reveals that as particle becomes bigger and darker especially in the centre and lighter at the outer part, suggesting the sphere shape. The minimum size is  $\sim 0.1 \mu\text{m}$  while maximum is almost  $\sim 2 \mu\text{m}$ . The boundary of NR particle becomes smear with SDS adsorption as shown in Figure 4.17(left).

As shown in Figure 4.15-4.23 the round smooth surface still preserved for the SDS admicelled NR particles, when PPy was admicelled polymerization on NR. It confirmed PPy-SDS-NR nanoparticles with a spherical structure similar to DBSA-oligopyrrole nanoparticles studied by Han.M et al.(2006)<sup>95</sup>. After washing to remove outer SDS layer the round shape was also seen, but its boundary is swollen into greater distance allowing PPy tiny globules (30-90nm) to reside. The PPy tiny globules was surrounded the NR particles and in the swollen region. This interesting to note that as PPy content increase ( $\geq 100\text{mM}$ ) the tiny globule packing becomes denser, as a result, the rough surface coating become smooth coating. This reveals the ultimate incorporation of PPy in NR at nanometer level. In addition, the dense packing of PPy globular should also attribute to the fast reaction when higher PPy content is used.



**Figure 4.15** Transmission electron microscope (TEM) imaged of PPy.



**Figure 4.16** Transmission electron microscope (TEM) image of the natural rubber latex and no OS (left), with OS (right)

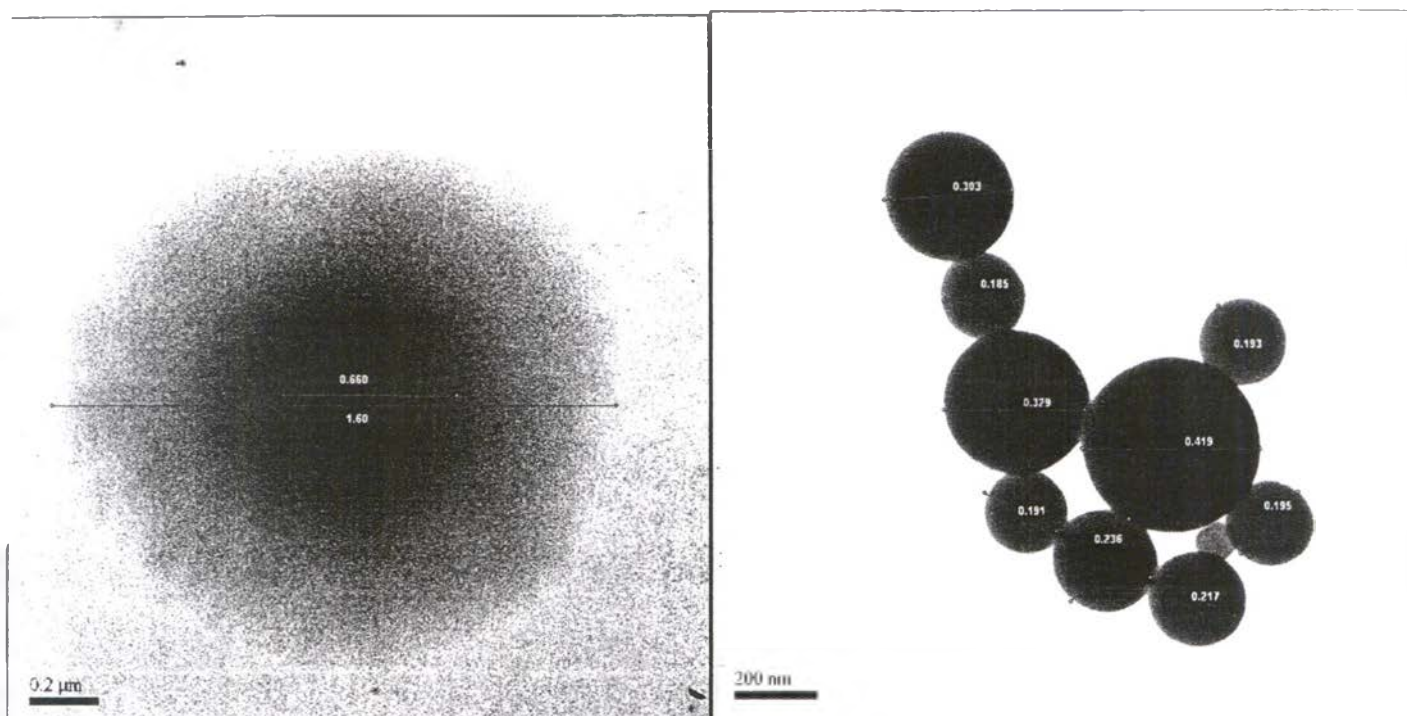


**Figure 4.17** Transmission electron microscope (TEM) image of the coated admicelled rubber with Sodium Dodecyl Sulfate (SDS) as a bilayer form, no OS (left), with OS (right).

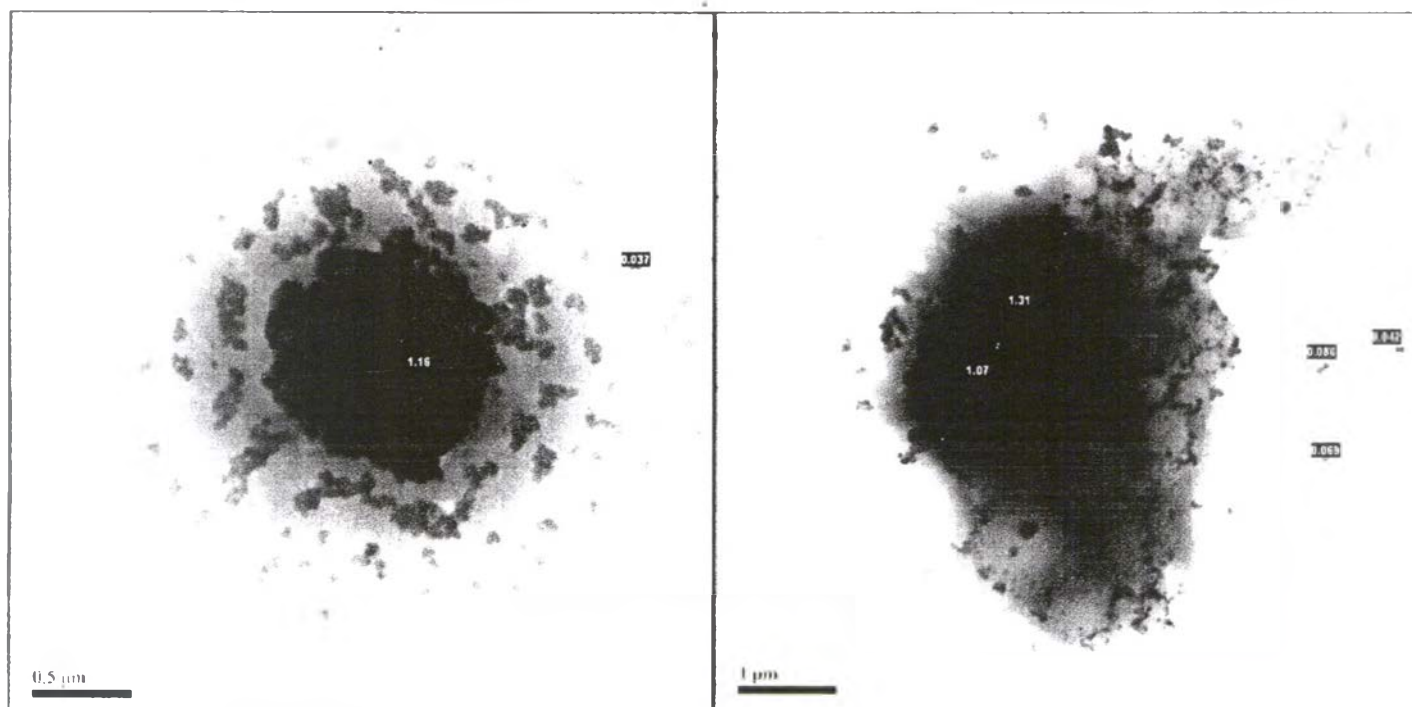


**Figure 4.18** Transmission electron microscope (TEM) image of the coated admicelled rubber (with 20 mM PPy) by using the electrochemical method.



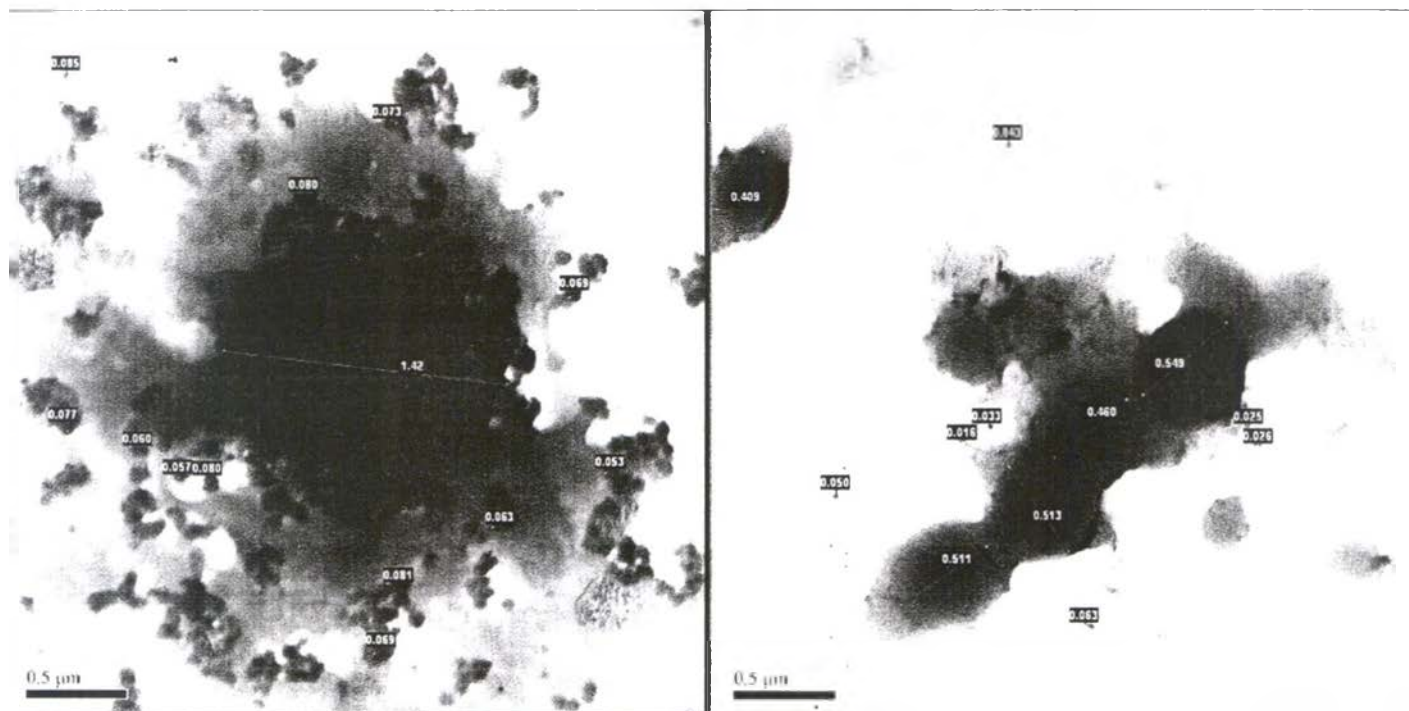


**Figure 4.19** Transmission electron microscope (TEM) image of the coated admicelled rubber (with 50 mM PPy) by using the electrochemical method.

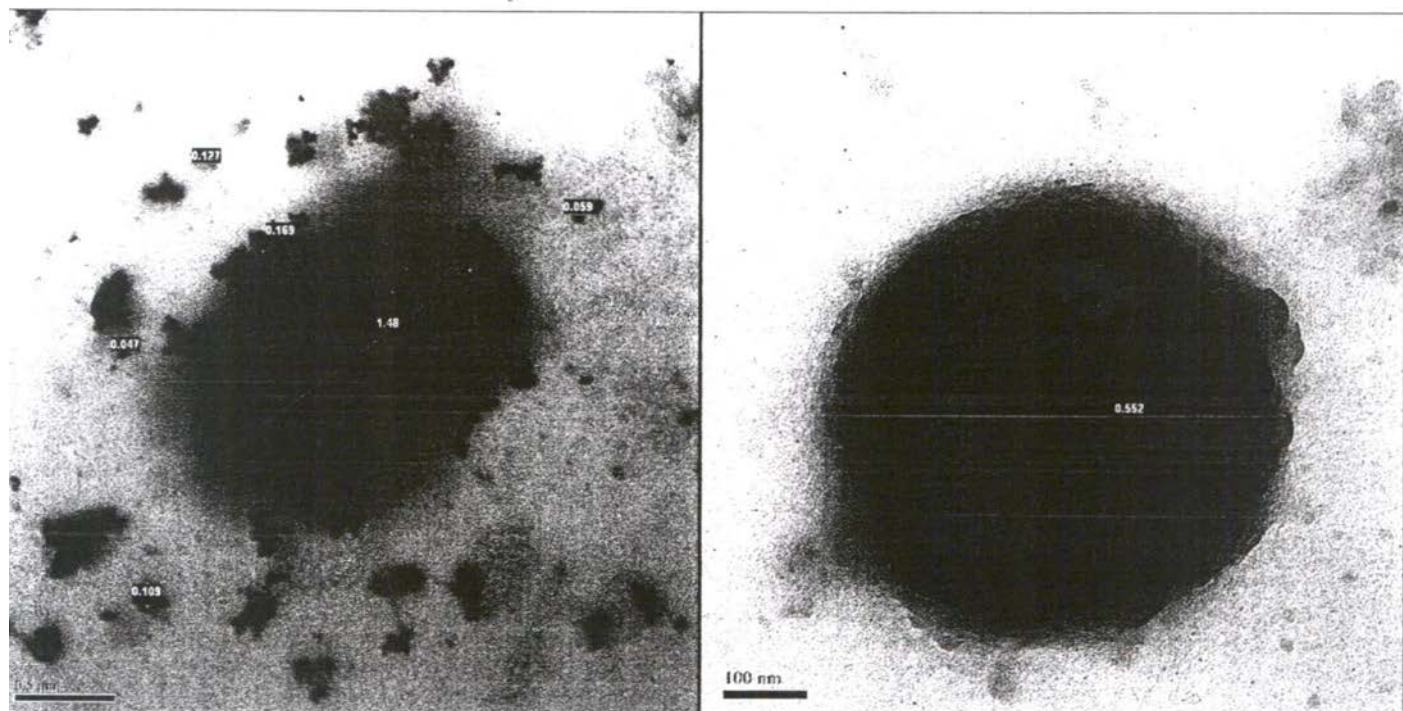


**Figure 4.20** Transmission electron microscope (TEM) image of the coated admicelled rubber (with 100 mM PPy) by using the electrochemical method.

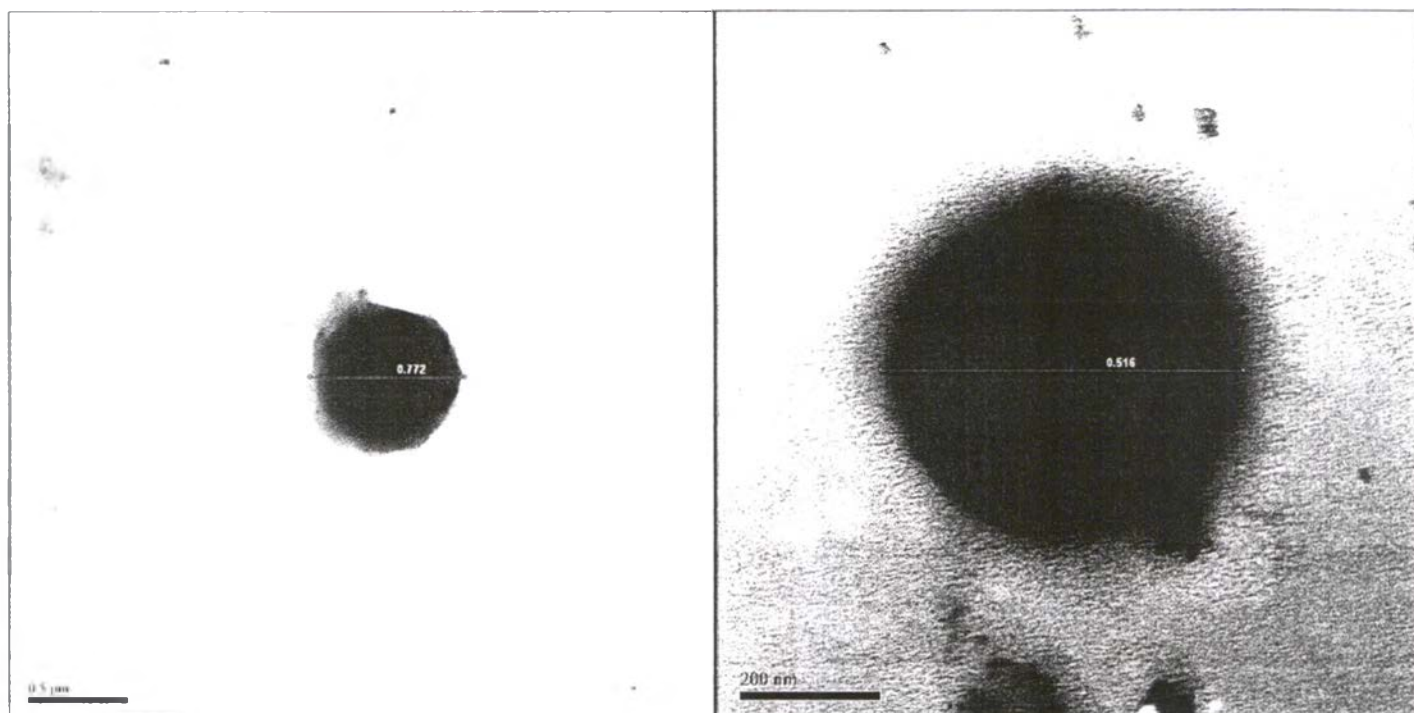


**Figure 4.21** Transmission electron microscope (TEM) image of the coated admicelled rubber (with 200 mM PPy) by using the electrochemical method.

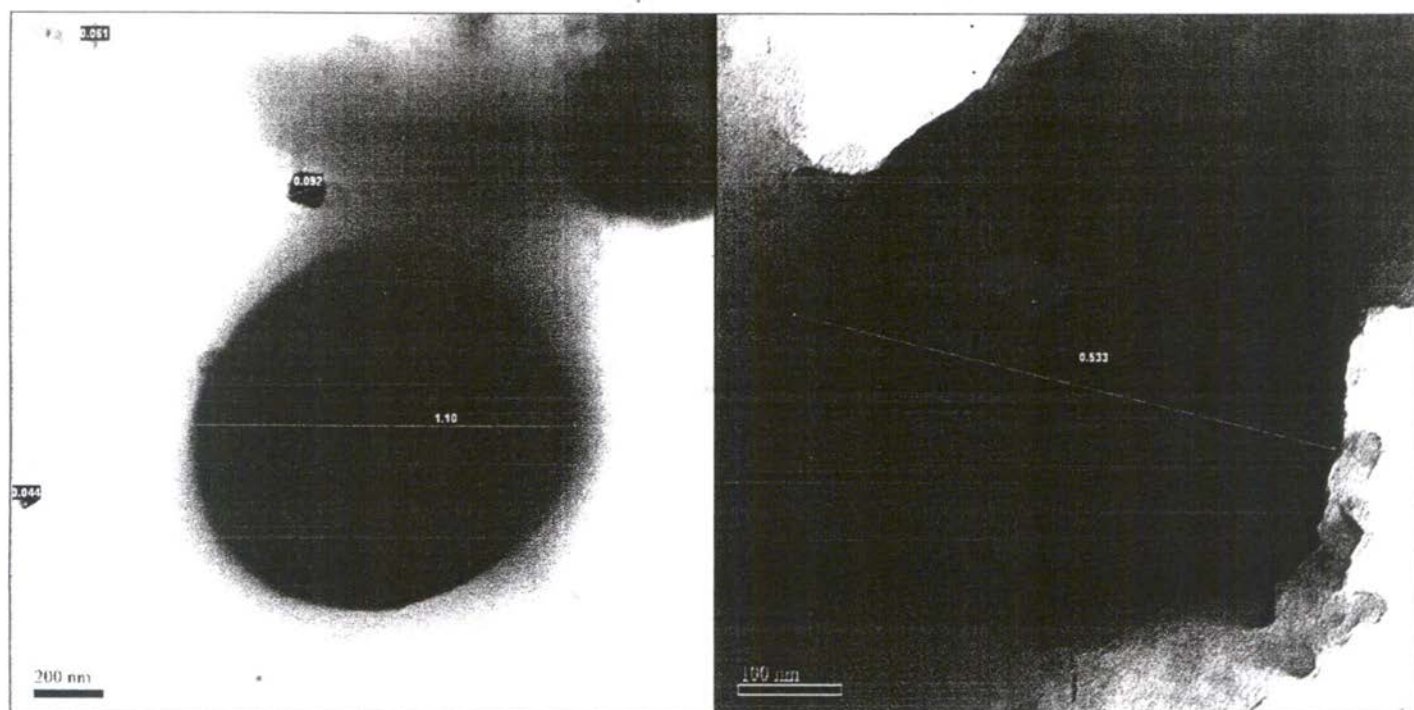


**Figure 4.22** Transmission electron microscope (TEM) of the coating admicelled rubber (with 500 mM PPy) by using the electrochemical method.

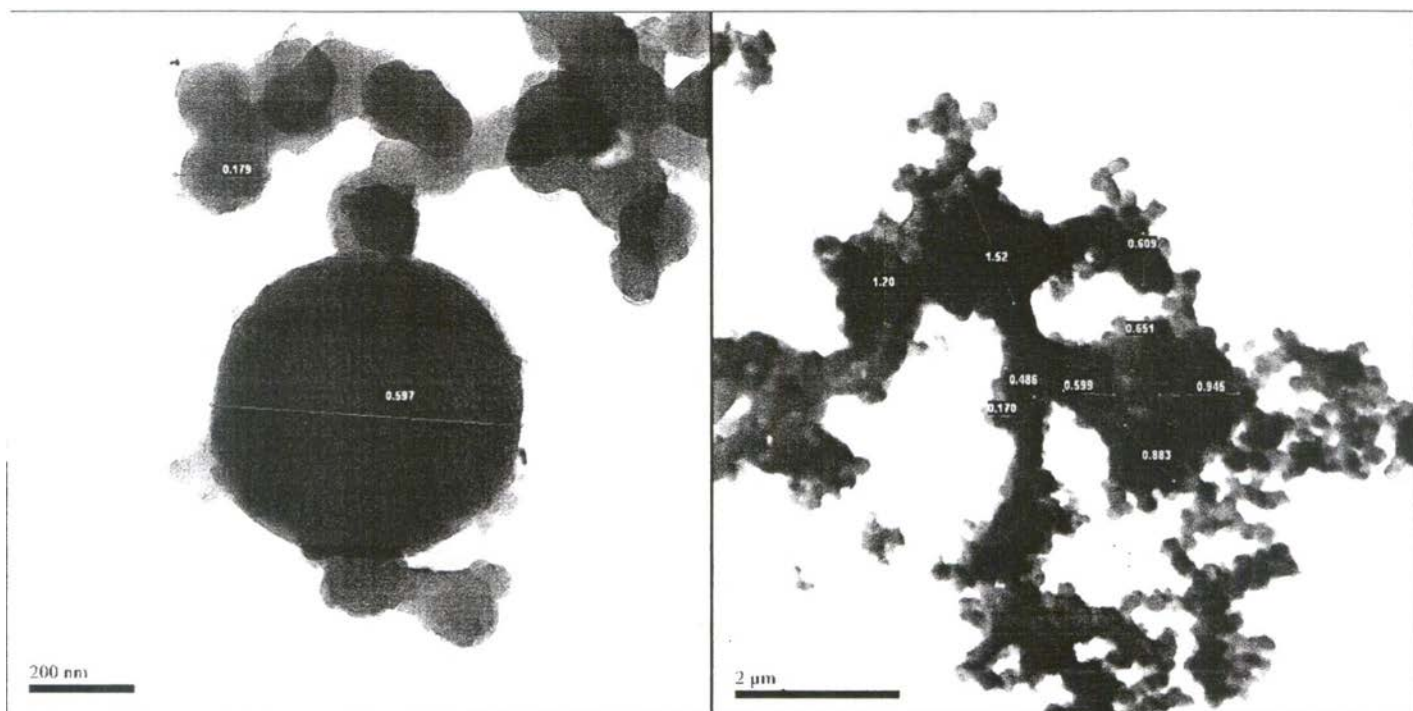


**Figure 4.23** Transmission electron microscope (TEM) image of the coated admicelled rubber (with 800 mM PPy) by using electrochemical method.

#### 4.4.6 Scanning Electron Microscopy

The morphologies of the PPy-admicelled rubbers were investigated by scanning electron microscopy. The SEM result can confirm the presence of polypyrrole. As observed in Figure 4.24, a grained texture is present and must be compared with the coarser cauliflower structure which is commonly found. The morphology of PPy in the presence of anionic surfactant was studied by Osmastova.M (2003)<sup>90</sup>. PPy-DBSNa showed significantly tiny particles (globules), and it showed that the presence of the anionic surfactant in the polymerization mixture strongly influenced the morphology of PPy preparation, which formed irregular aggregates whereas NR exhibited the smooth surface without any coating as shown in Figure 4.25.

The SEM micrographs of the admicelled rubbers with different PPy concentrations reveal the round shape of rubber particles with even coating of PPy over the particles. The sample with 20 mM PPy shows latex particles coated by a PPy layer as a core-shell structure where NR particles are the core and PPy is the shell, and it becomes a continuous or matrix. The samples with 50, 100, 200, 500, and 800 mM of PPy clearly show the coating of PPy on each latex particle individually, which is shown in Figures 4.26-4.31. They also show no phase separation between the PPy and the NR. This suggests a high level of dispersability of rubber particles and PPy. The average particle diameter was estimated to be between 0.6-1.6  $\mu\text{m}$ , or approximately the same as the value determined by the particle size analyzer. This also reveals the very fine nanometer thickness of the PPy shell.



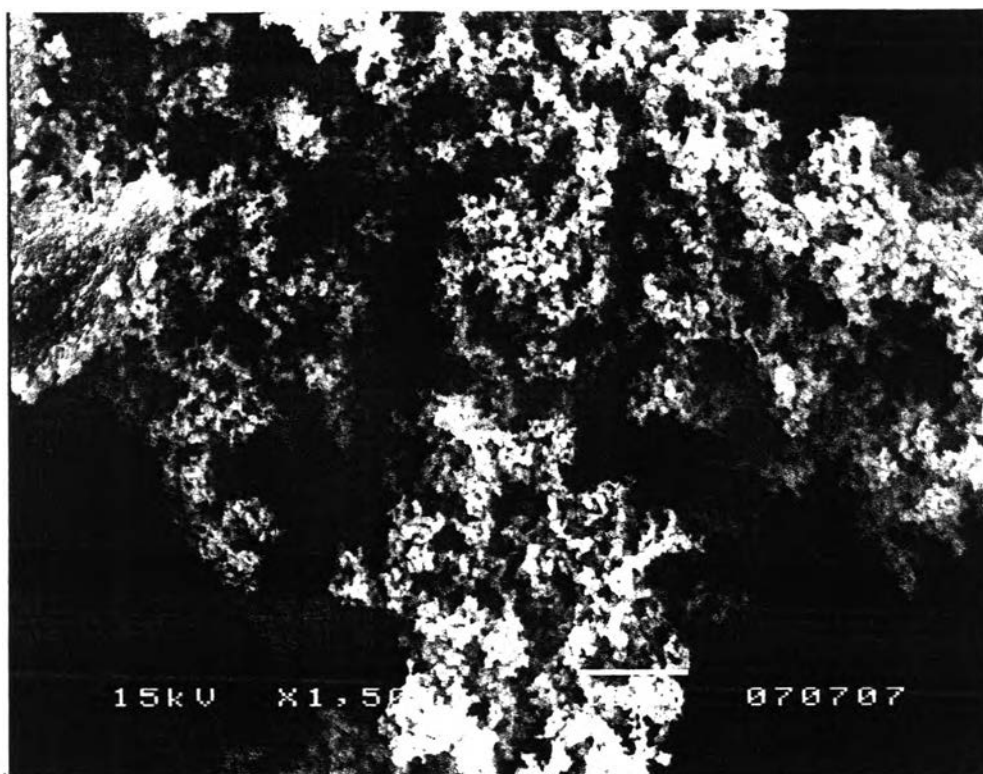


**Figure 4.24** Scanning electron micrograph of the coat polypyrrole by using electrochemical method; magnification 1,500/15 kV

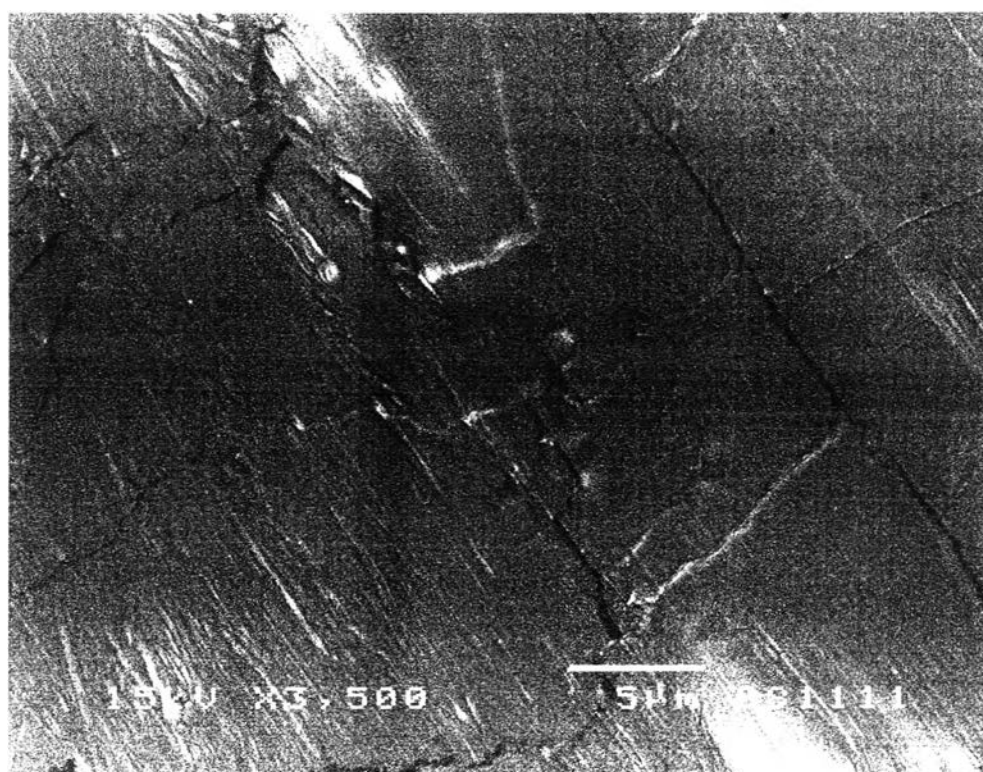


**Figure 4.25** Scanning electron micrograph rubber magnification 1,500/15 kV

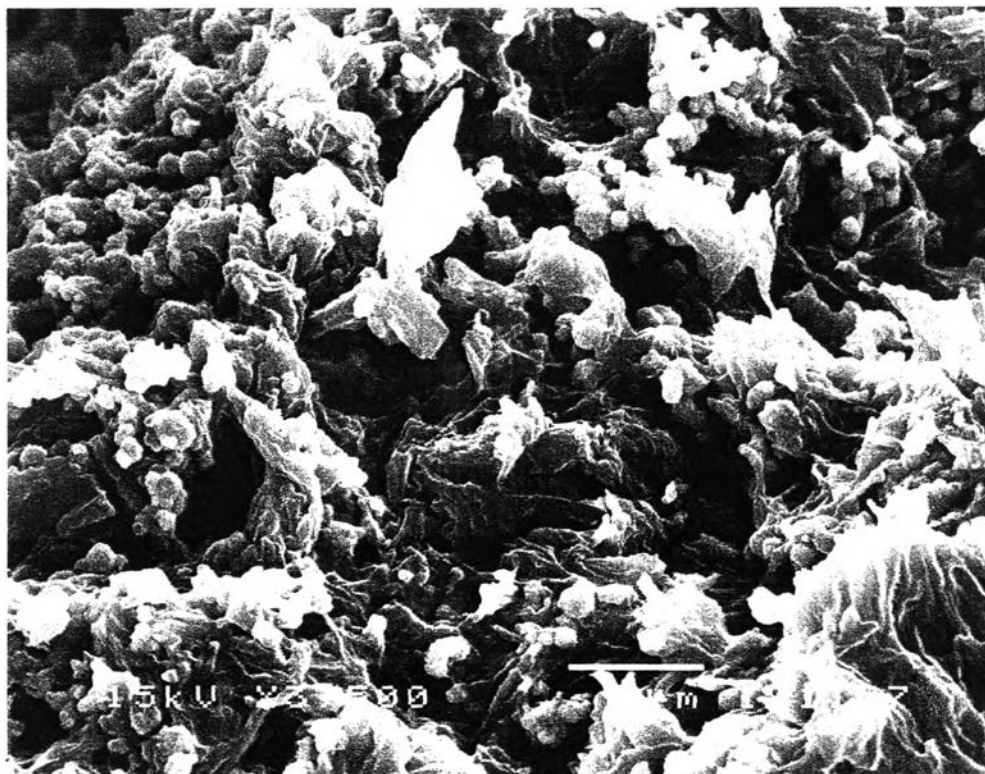


**Figure 4.26** Scanning electron micrograph of the coated admicelled rubber (with 20 mM PPy) by using electrochemical method; magnification 1,500/15 kV.

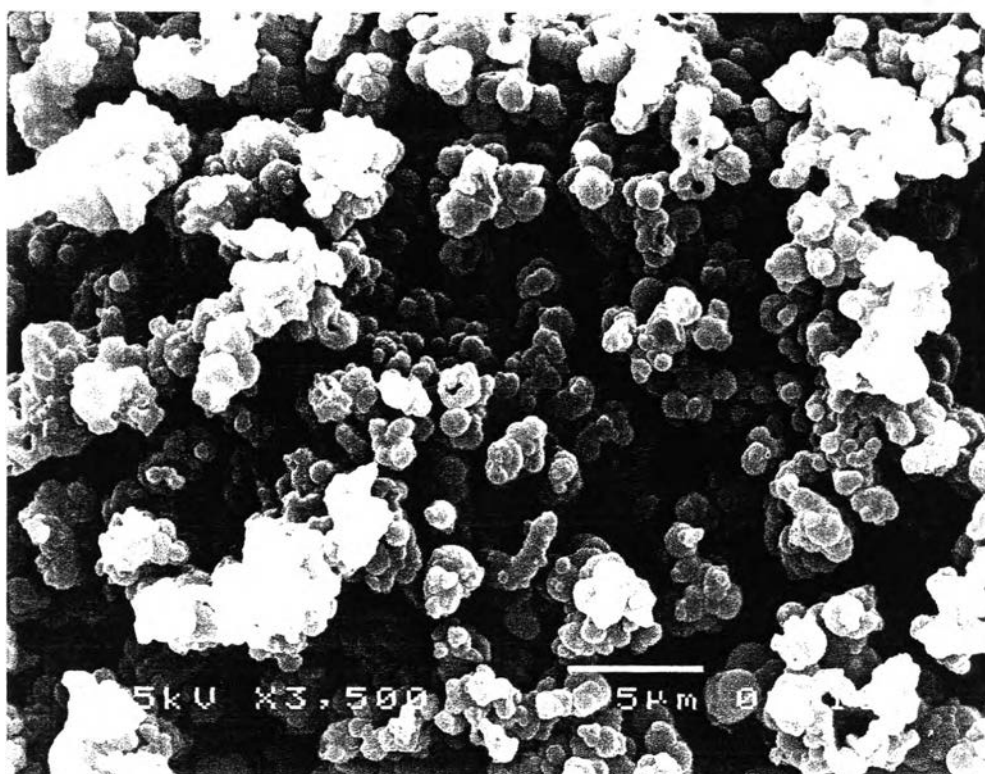


**Figure 4.27** Scanning electron micrograph of the coated admicelled rubber (with 50 mM PPy) by using electrochemical method: magnification 1,500/15 kV.

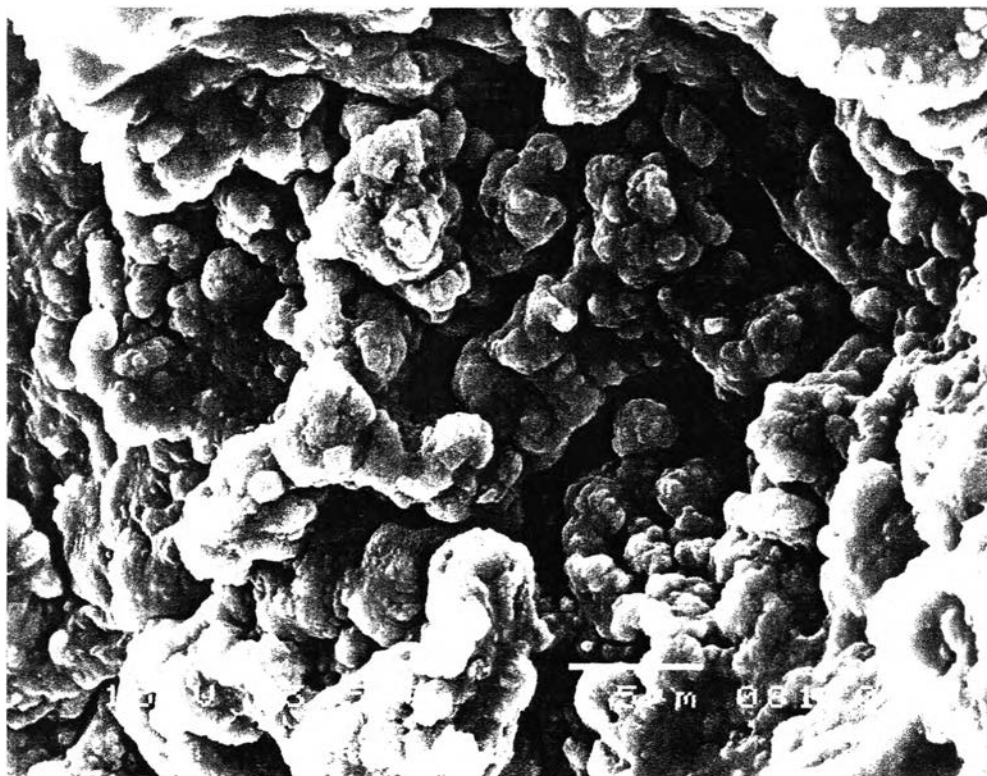


**Figure 4.28** Scanning electron micrograph of the coating admicelled rubber (with 100 mM PPy) by using electrochemical method magnification 1,500/15 kV.

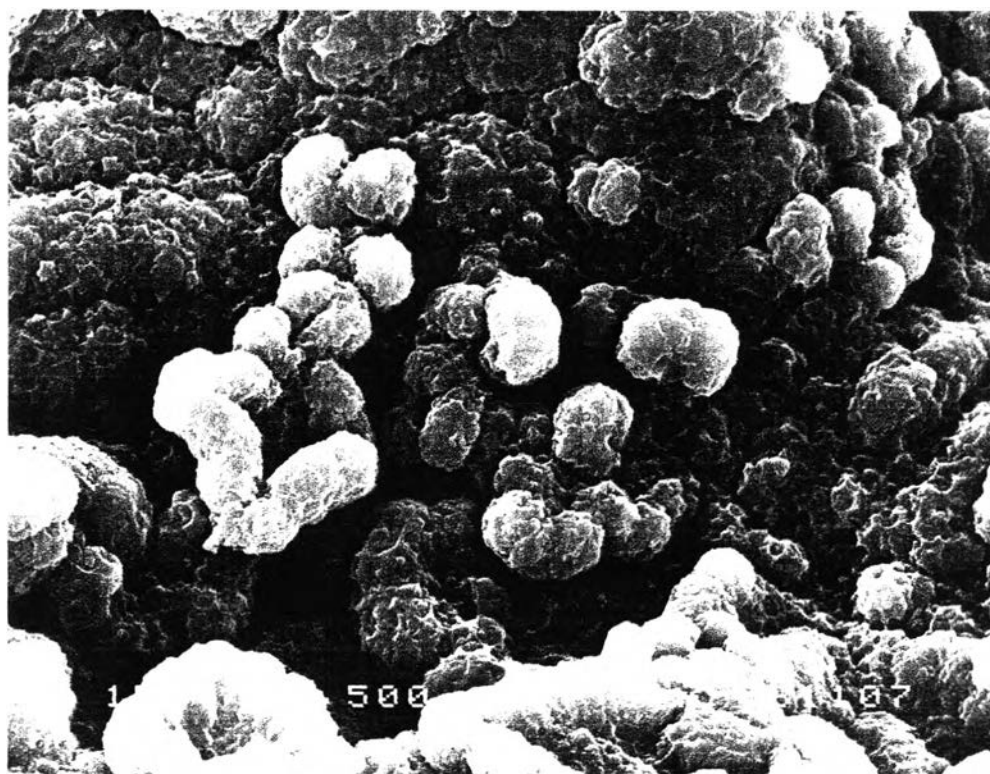


**Figure 4.29** Scanning electron micrograph of the coated admicelled rubber (with 200 mM PPy) by using electrochemical method: magnification 1.500/15 kV.



**Figure 4.30** Scanning electron micrograph of the coated admicelled rubber (with 500 mM PPy) by using electrochemical method; magnification 1,500/15 kV.

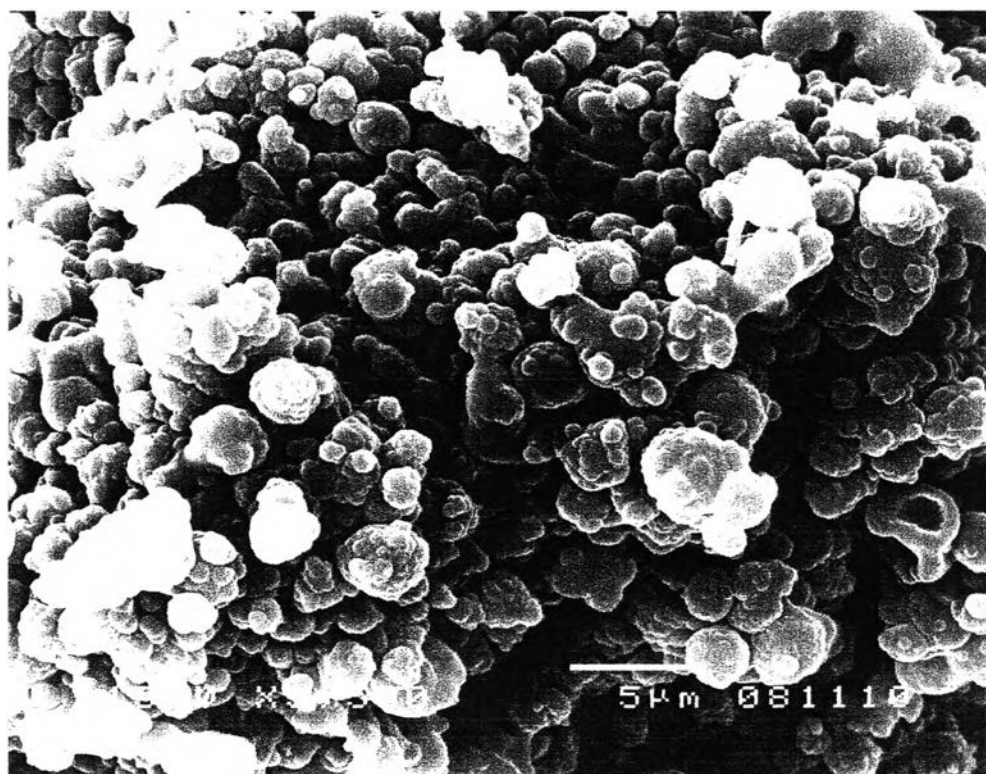


**Figure 4.31** Scanning electron micrograph of the coated admicelled rubber (with 800 mM PPy) by using electrochemical method; magnification 1,500/15 kV.



#### 4.4.7 Thermogravimetric Analysis (TG-DTG)

TG-DTG patterns of PPy-NR composites are shown in Figures 4.32 to 4.37. It can be seen from the TGA curve that 10% weight loss in the range of 100-250°C is due to the evaporation of physically absorbed water and loss of some surfactant and product surface. NR shows the major decomposition at 373.6°C and PPy starts to degrade from 204.9°C (Figure 4.32). Then the main mass loss is observed at 260.3°C because of rearrangement and degradation of the side chain (M.Han,2006)<sup>95</sup>. The significant weight loss of the admicelled rubbers shows at around 369.4 to 374.5°C. The decomposition temperature (Peak temperature from TGA) of the admicelled rubber increases with higher amount of PPy. They lose about 80-90% of their weight between 345 and 525°C as shown in Figure 4.33.

This suggests that the admicelled rubbers begin to lose weight at similar decomposition temperature as that of NR (Figure 4.34) and they also show the shift of major decomposition of pure PPy to higher temperature ( $T_d$  of rubber = 373.6°C,  $T_d$  of PPy = 260.3°C,  $T_d$  of the admicelled rubbers = 369.4 to 374.4°C), compared to the result of Shen Y. and Wan M. (1998)<sup>6</sup>, the decomposition temperature of PPy is at 217°C and 180°C (Jang KS,2004)<sup>4</sup>. The DTG a curve of the admicelled rubbers follow the shape of the DTG a curve of pure rubber during heating from 30 to 400°C. The reason is that the main composition is NR (%wt. of PPy added is about 2-51% : Table A2), indicating that rubber is a dominant factor affecting the thermal stability of the admicelled rubbers. Moreover, this decomposition can attribute to the swollen NR that acts as binder between admicelled NR particles. The second decomposition goes on as a shoulder at high temperature 400-500 °C where about 40-50 %wt of admicelled NR are now decomposed.

The decomposition temperatures were also ended at higher temperature (521.1°C) than that of pure rubber (471.9 °C) as shown in the Table 4.9. higher ending temperature with higher PPy content (Figure 4.36). The higher the PPy content, the slower the samples start to degrade. This attribute to PPy coating that shields the core NR from early decomposition. This fact also supports that coating PPy encapsulating NR by admicellar polymerization can improve the thermostability of natural rubber.

The curves also demonstrate that char yields of the admicelled rubbers increased from 1% of pure rubber to 3.53 – 59.46% related to the content of PPy added. The residual content of samples with PPy 20 mM (3.53 %wt.) are about 4.9% ; PPy 50 mM (8.41%wt.),11.1 % ; PPy 100 mM (15.47%wt.),16.8 % ; PPy 200 mM (26.83%wt.),17.9 %; PPy 500 mM (47.82%wt.),19.2%; and PPy 800 mM (59.46%wt.),22.3 %. These indicate that an increase of PPy content enhanced the residue remaining (the residual content of pure PPy is 66.58%), Figure4.37.

**Table 4.9** Degradation temperature of the admicelled rubbers

Sample	Onset Temperature	End point Temperature	Peak temperature	residual content (%)
Rubber	351.6	471.9	373.6	1.1
20	348.9	481.5	369.4	4.9
50	347.8	485.3	368.6	11.1
100	349.2	493.9	370.2	16.8
200	352.8	496.6	373.5	17.9
500	353	505.9	374.5	19.2
800	352.2	521.1	374.4	22.3
PPY	204.9	579.3	260.3	66.58

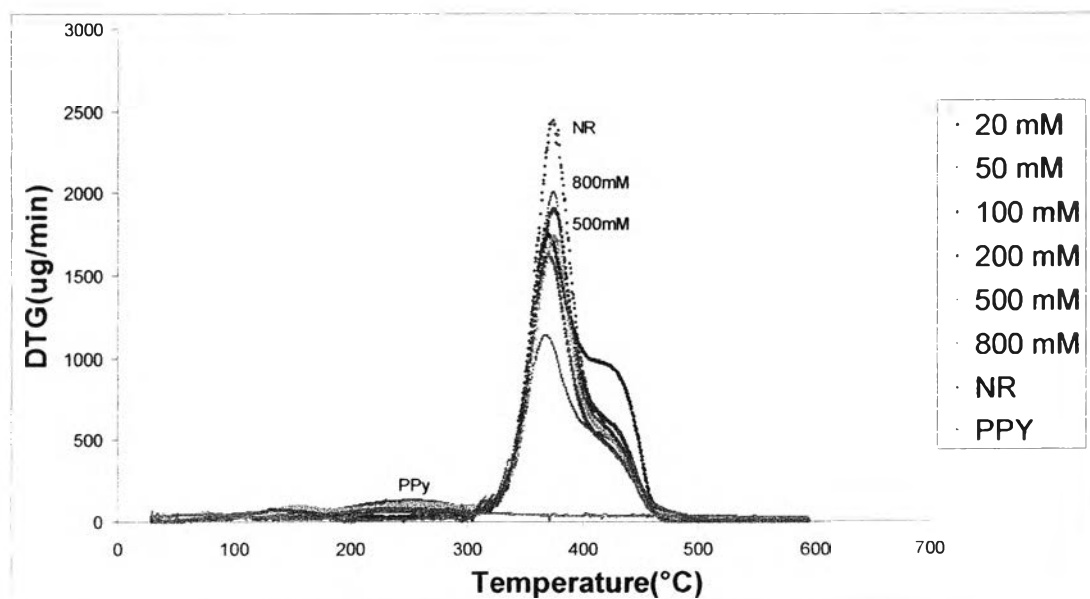


**Figure 4.32** DTG thermograms at 10 °C/min nitrogen atmosphere of admicellar rubbers with SDS by using electrochemical methods.

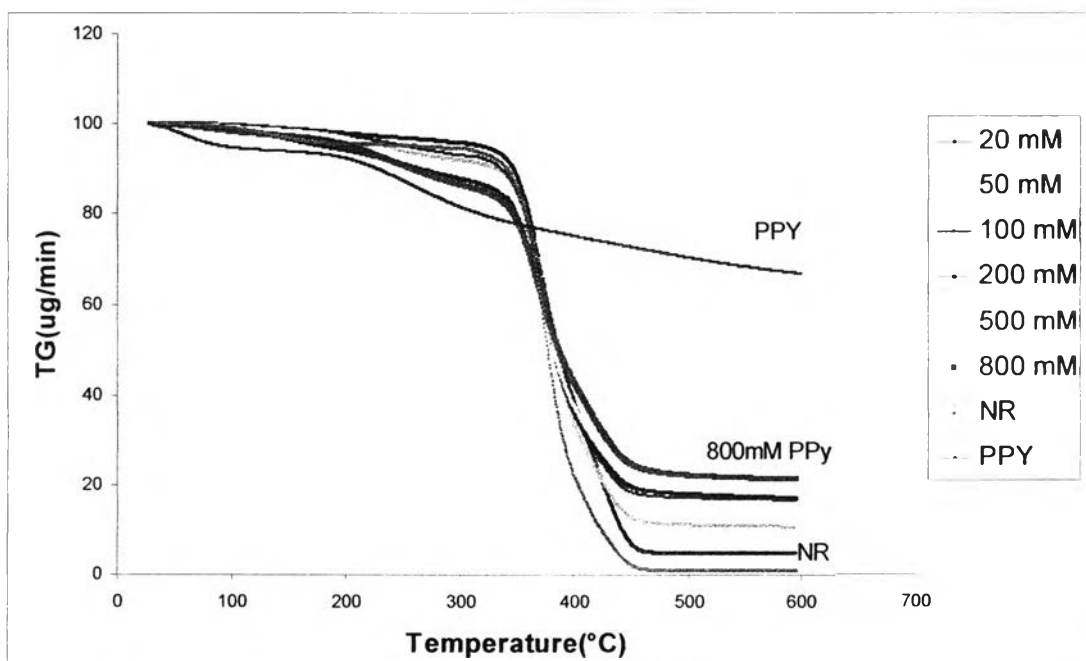


**Figure 4.33** Thermogravimetric analysis thermograms at 10°C/min in nitrogen atmosphere of admicellar rubbers with SDS by using electrochemical methods.

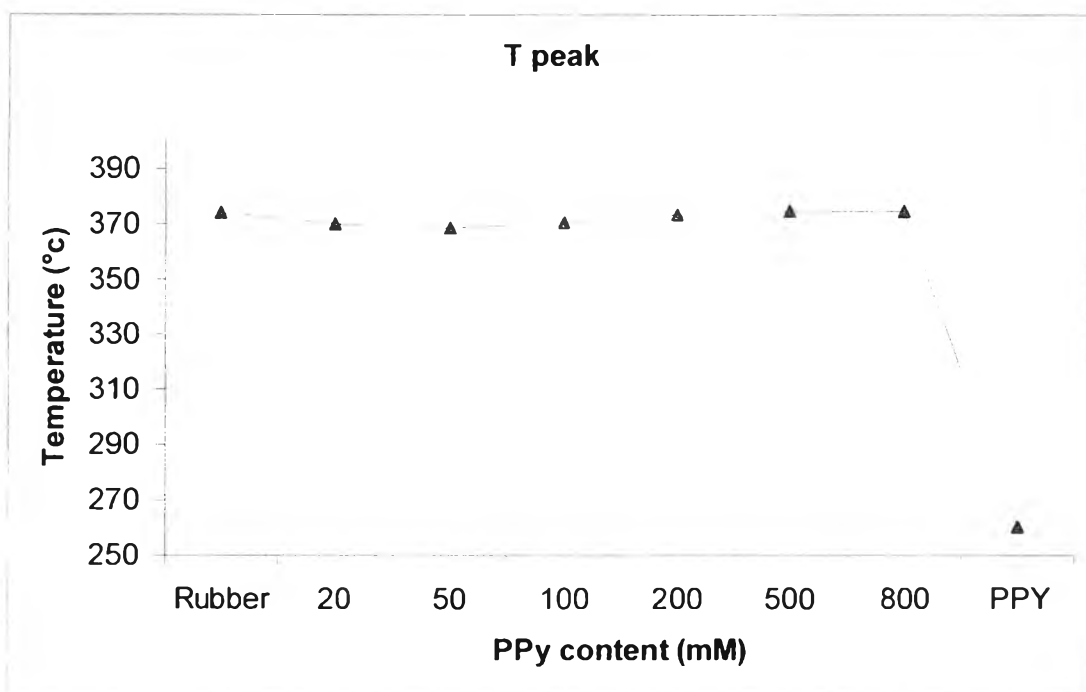


**Figure 4.34** Thermogravimetric analysis thermograms at 10°C/min in nitrogen atmosphere of admicellar rubbers with SDS by using electrochemical methods.

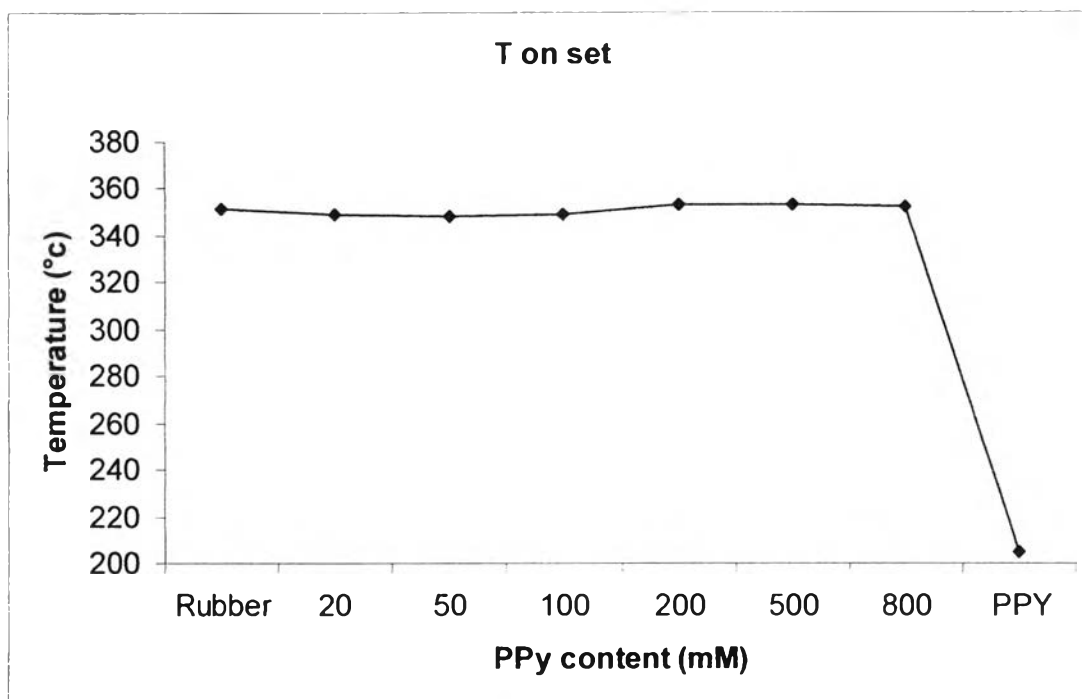


**Figure 4.35** Thermogravimetric analysis thermograms at 10°C/min in nitrogen atmosphere of admicellar rubbers with SDS by using electrochemical methods.

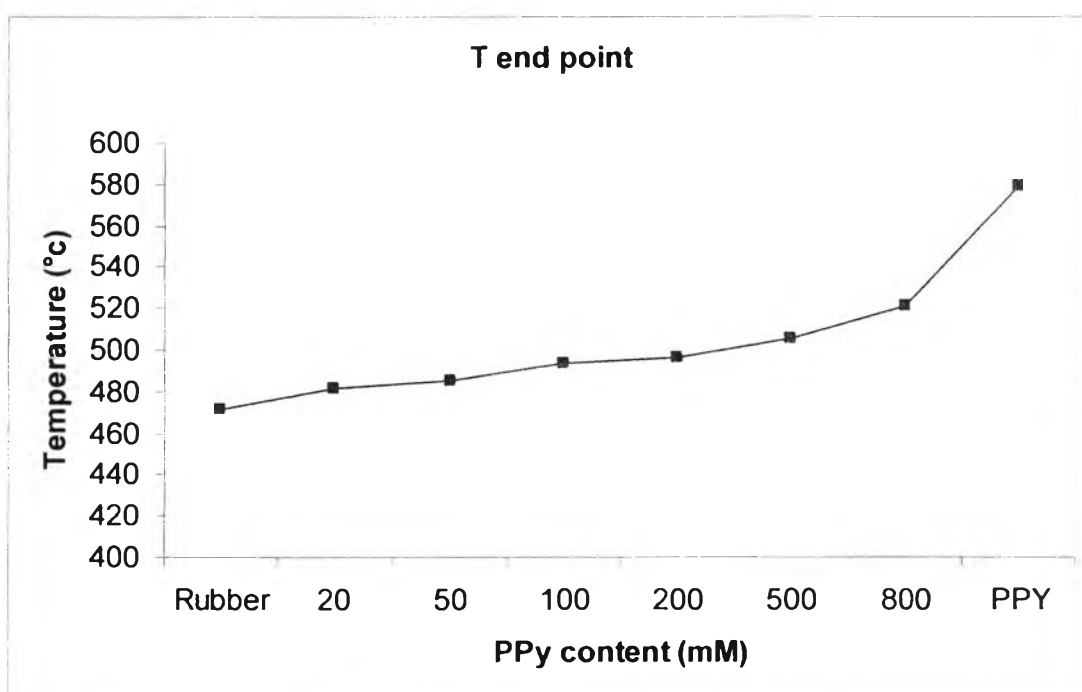


**Figure 4.36** Thermogravimetric analysis thermograms at 10°C/min in nitrogen atmosphere of admicellar rubbers with SDS by using electrochemical methods.



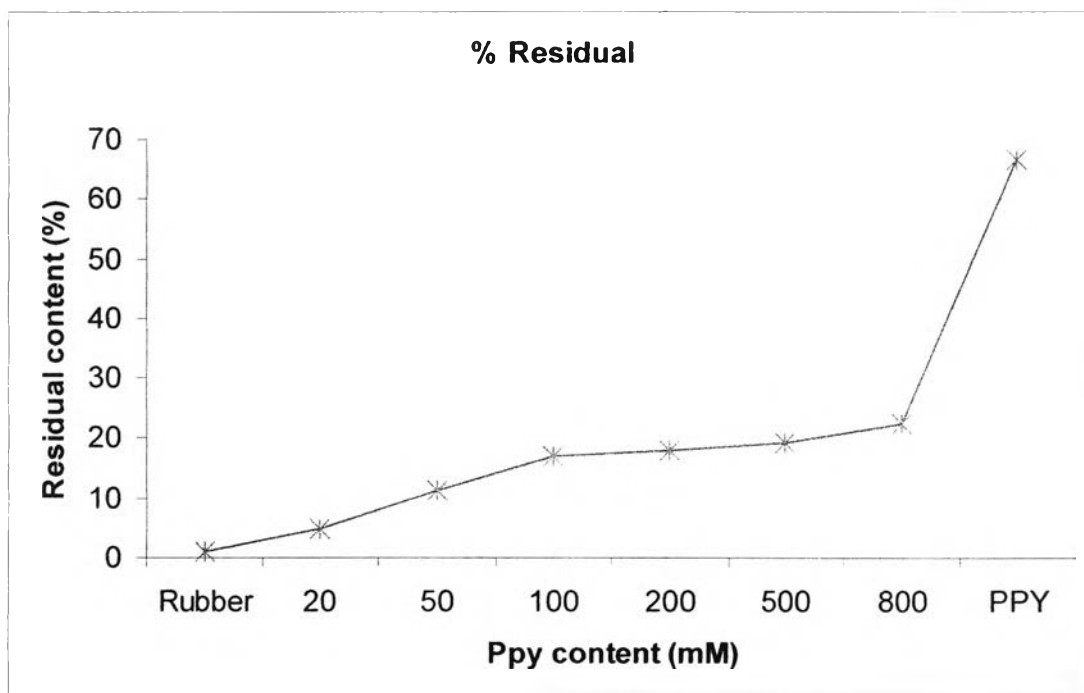


**Figure 4.37** Thermogravimetric analysis thermograms at 10°C/min in nitrogen atmosphere of admicellar rubbers with SDS by using electrochemical methods.

## 4.4.8 Mechanical Properties Measurement

### 4.4.8.1 Lloyd Universal Testing Machine

The mechanical properties of the admicelled latex films were determined using a Lloyd Universal Testing Machine with a crosshead speed of 50 mm/min, and gauge length of 50 mm, under room temperature. The tests followed ASTM D882-91. The effects of pyrrole concentration on the mechanical properties of admicelled rubber films are shown in Figures 4.38-4.42. Table 4.10 shows that the pure NR film was soft, tough, and highly elastic, with high elongation at break (311.75 %), a high value for work to break (0.672 J), but low tensile strength at break ( $4.8657 \times 10^5$  Pa). Conversely the mechanical properties of PPy admicelled NR change from soft and elastic to hard and brittle, depending on the amount of pyrrole monomer incorporation. Increasing the concentration of PPy to NR, leads to a harder and more brittle material. The tensile strength at break can be improved from  $4.8657 \times 10^5$  Pa to  $18.792 \times 10^5$  Pa (Figure 4.39). The maximum tensile strength is 3 times higher than that of natural rubber. This value is lower than the result of J.Y. Lee (1995)<sup>157</sup> where the tensile strength of doped polypyrrole films with DBSA and DS was 17 and 68.5 MPa, respectively. However, it differs in their set up parameters such as crosshead speed (1mm/min) and gauge length (3cm). This is also lower when compared to the chemical method by using the admicellar technique around 10 times. However, the elongation at break decreased from 180.95 to 89 %. Figure 4.40 with increasing PPy content was also observed. It was similar trends from work to the break value from 0.55 to 0.24J (Figure 4.41). The study of mechanism behavior of PPy incorporated with  $\text{FeCl}_3$  by Mano V. et al (1996)<sup>112</sup> showed an elongation at break of pure PPy lower than 5% and breaking without drawing. Thus, the higher the PPy content in the admicelle rubbers, the lower the elongation at break is. Indeed, the reason for lower mechanical properties between the chemical method and the electrochemical method is the incorporation of an initiator such as  $\text{FeSO}_4$  and  $\text{FeCl}_3$  into the composite. This can be given higher interactions between molecules and improved its properties such as ductility and toughness Mano V. et al (1996)<sup>112</sup>. Furthermore, the young's modulus is built up from 1.1-2.85 MPa with increasing PPy content revealing the higher stiffness as shown in Figure 4.42.

**Table 4.10** Composition and properties of PPy/NR obtained by admicellar technique by Lloyd universal testing machine

Sample (mM)	Elongation at break (%)	Tensile strength at break (Mpa)	Work to Break (J)	Young's modulus (MPa)
NR	311.75 ± 6.23	0.48657 ± 0.002	0.6724 ± 0.013	0.1667 ± 0.013
20 (A2)	180.95 ± 9.05	0.56688 ± 0.006	0.5571 ± 0.027	1.11 ± 0.022
50 (A5)	144.91 ± 10.14	0.98323 ± 0.033	0.5110 ± 0.086	1.25 ± 0.025
100 (A10)	118.83 ± 11.18	0.92941 ± 0.018	0.4912 ± 0.049	1.60 ± 0.032
200 (A20)	90.06 ± 9.01	0.9441 ± 0.0192	0.3824 ± 0.038	2.00 ± 0.040
500 (A50)	73.47 ± 16.16	1.3561 ± 0.0190	0.2623 ± 0.018	2.50 ± 0.050
800 (A80)	88.87 ± 6.22	1.8792 ± 0.0266	0.2413 ± 0.016	2.85 ± 0.057

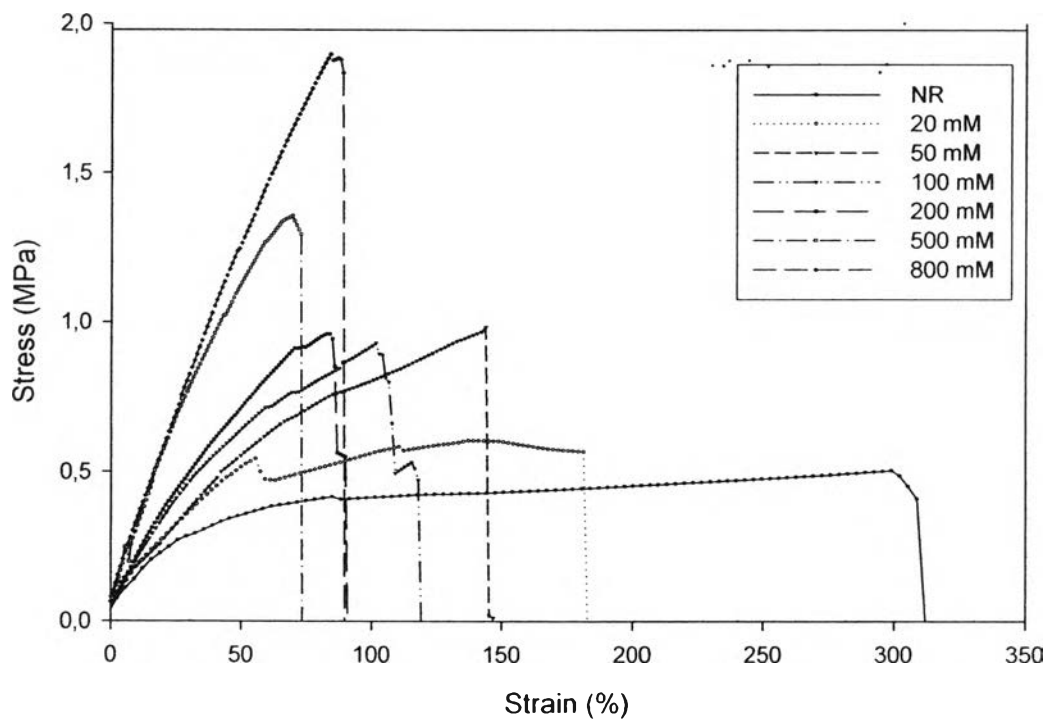


**Figure 4.38** Effect of polypyrrole concentration on the stress-strain curves of admicelled rubber.

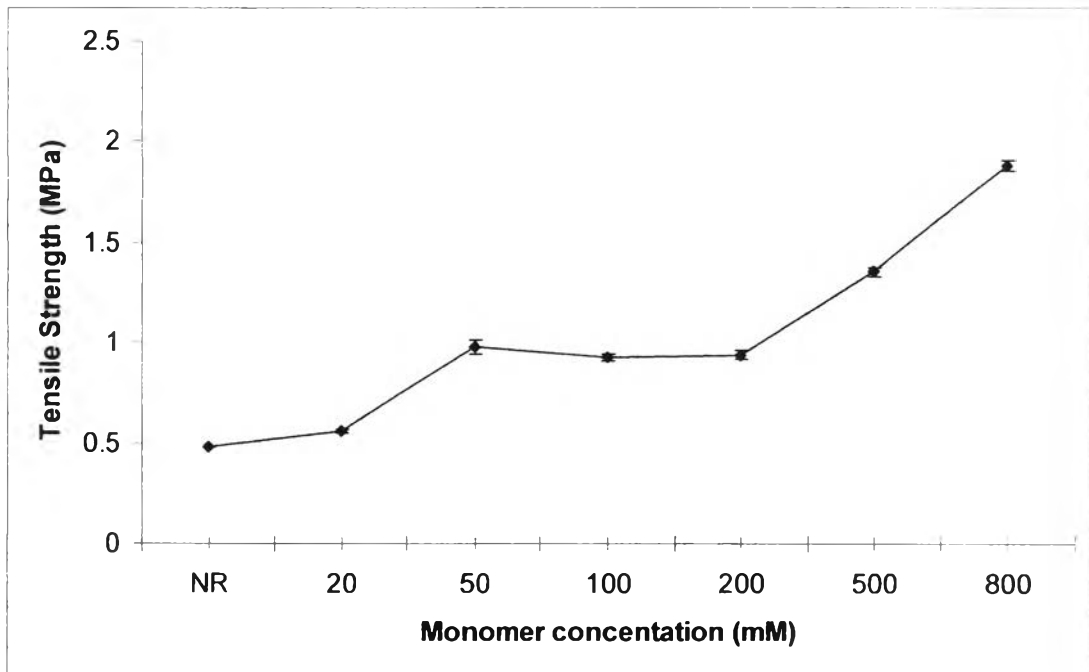


Figure 4.39 Tensile strength varying the concentration of polypyrrole.

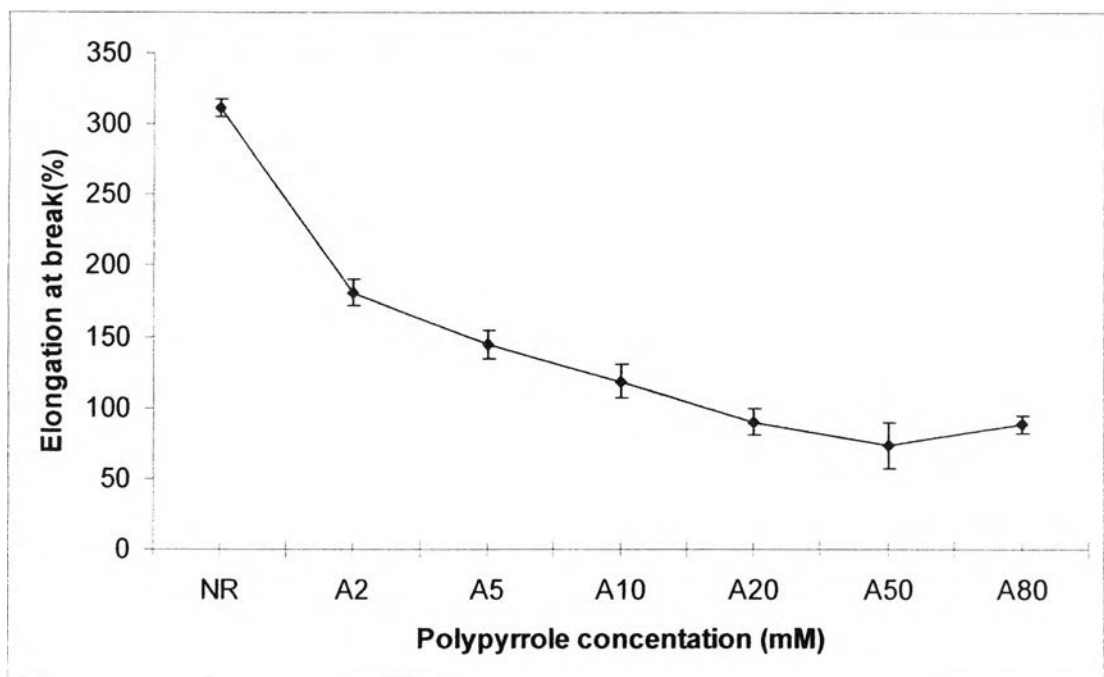


Figure 4.40 Elongation varying the concentration of polypyrrole

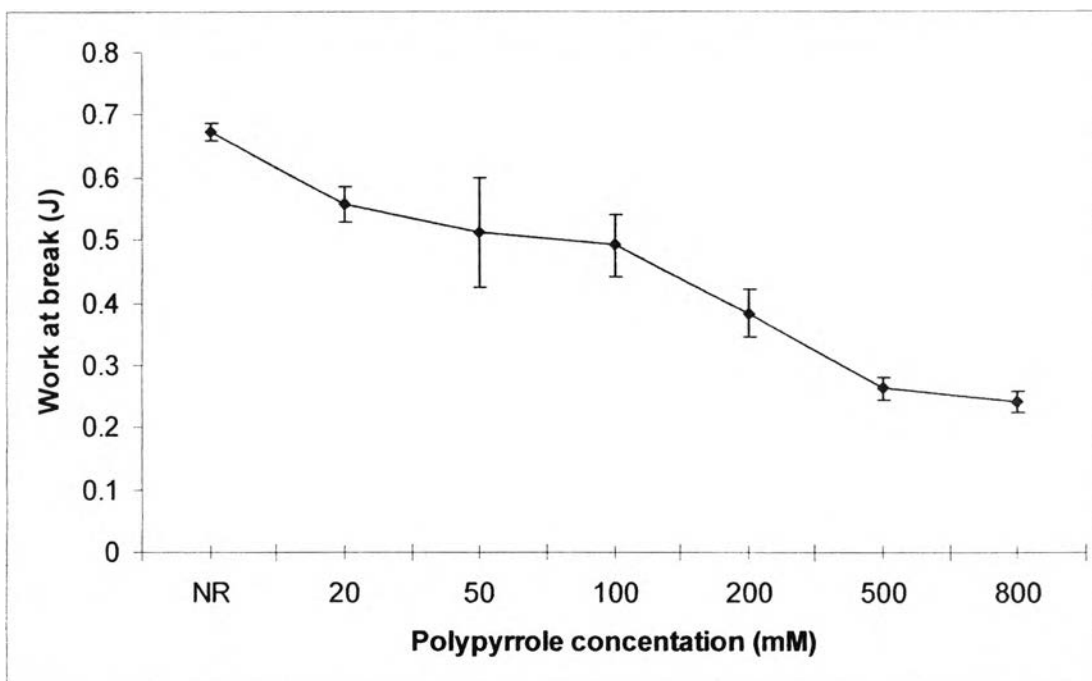


Figure 4.41 Effect of polypyrrole concentration on the energy at break.

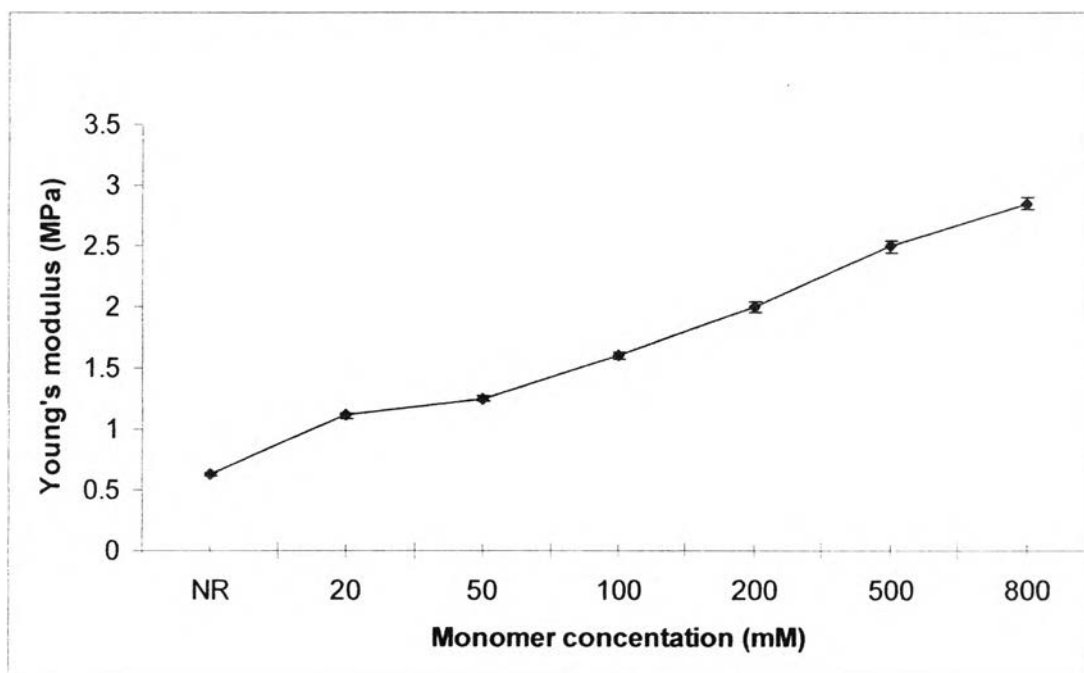


Figure 4.42 Effect of polypyrrole concentration on Young's modulus

#### 4.4.8.2 Instron Universal Testing Machine

The mechanical properties were also confirmed by using Instron UTM testing with a crosshead speed 50 mm/min a gauge length of 13 mm, and a load cell of 100 kN under room temperature. The test was repeated 5 times. The dumbbell shape, which has thickness larger than 3 mm, was cut by using a pneumatic punch following ASTM D638M-91a. The tensile tests showed higher stiffness of the admicelled rubbers than that of natural rubber (Figures 4.43-4.47). The tensile strength of uncrosslinked natural rubbers (thickness around 3 mm) is close to 1.3 MPa and the tensile strength of the admicelled rubbers is around 1-3 MPa as shown in Figure 4.44. The maximum tensile strength of the admicelled rubbers is 3.51 MPa, which is higher than the testing by using the Lloyd Universal Testing Machine because of the difference in their thickness and size. This can be confirmed by Demirhan .E et al.(2006)<sup>118</sup> who studied the physical properties of vulcanized SBR-1712 by adding carbon black such as the tensile strength is around 5-14 MPa. The results showed the similar trends which rubber reduces stiffness of conductive composite and it results in such a reasonable tensile strength. The elongation at break of NR is about 831% while those of the admicelled rubbers are lower around 221-664%; increasing PPy content shows more brittleness (reducing elongation) due to the rigidity of PPy (Table 4.11 and Figure 4.45). The study of the mechanical behavior of PPy 38%wt in Styrene-Butadiene-Styrene (SBS) by Sun Y. et al. (1995)<sup>117</sup> showed the less elongation at break, around 305-354%. The work to the break results also show the brittleness of admicelled NR developed with increasing PPy content (Figure 4.46). Surprisingly, young modulus increased from 0.3 MPa (NR) to 0.17 MPa at 800 mM, PPy showing the increase in stiffness of the admicelled NR with PPy content. It decreased from 0.5 to 1.0 J as higher amount of polypyrrole as shown in Figure 4.47.

**Table 4.11** Composition and properties of PPY/NR were obtained by admicellar technique Instron Universal Testing Machine

Sample (mM)		Elongation at break (%)	Tensile strength at break (MPa)	Work to Break (J)	Young's modulus (Mpa)
NR		831.46 ± 16.63	1.3011 ± 0.026	1.0181 ± 0.020	0.333 ± 0.006
PPY	20 A2	655.28 ± 32.21	1.5021 ± 0.075	0.9984 ± 0.049	0.266 ± 0.005
	50 A5	521.94 ± 36.53	1.7012 ± 0.289	1.0593 ± 0.180	0.401 ± 0.001
	100 A10	392.34 ± 39.23	1.9839 ± 0.198	0.6848 ± 0.068	0.533 ± 0.011
	200 A20	380.13 ± 38.01	2.0512 ± 0.205	0.6746 ± 0.067	0.60 ± 0.012
	500 A50	226.86 ± 49.90	3.0112 ± 0.211	0.5654 ± 0.039	1.333 ± 0.027
	800 A80	221.67 ± 15.51	3.5175 ± 0.246	0.4581 ± 0.032	1.667 ± 0.033

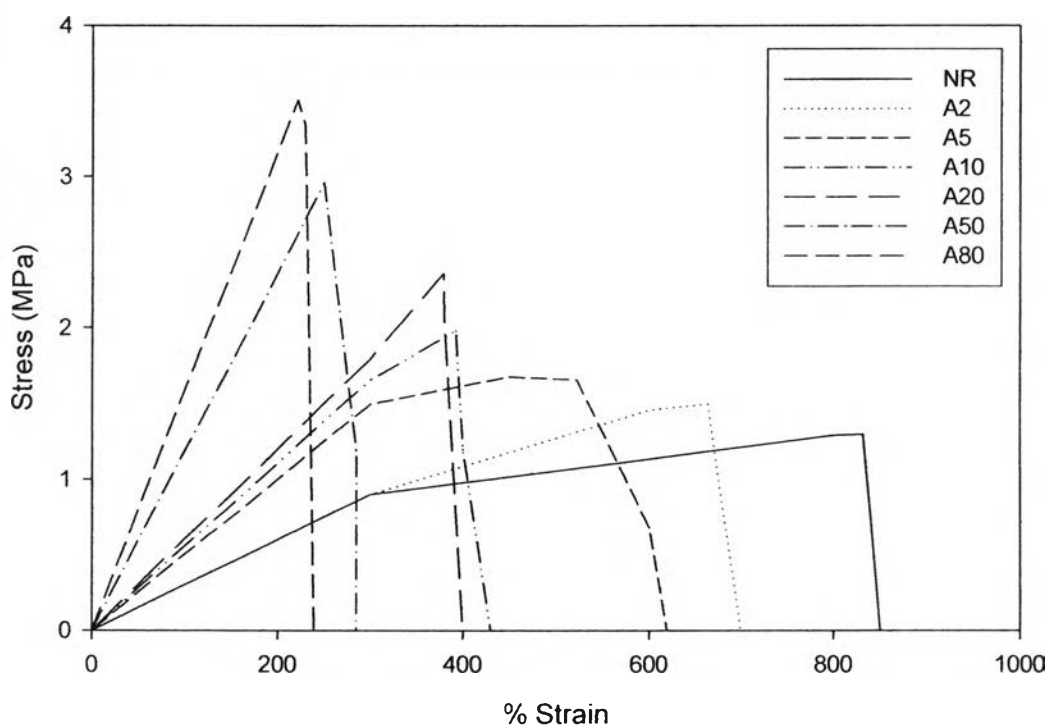


**Figure 4.43** Effect of polypyrrole concentration on the stress-strain curves of conductive rubber.

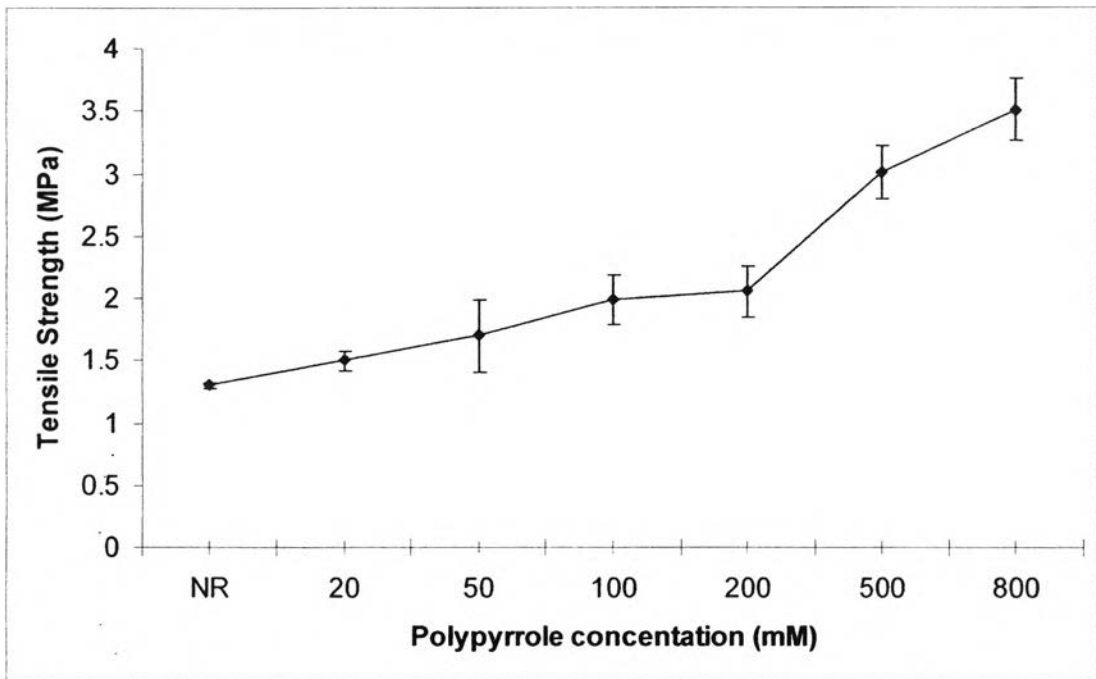


**Figure 4.44** Tensile strength varying the concentration of polypyrrole (Instron machine).

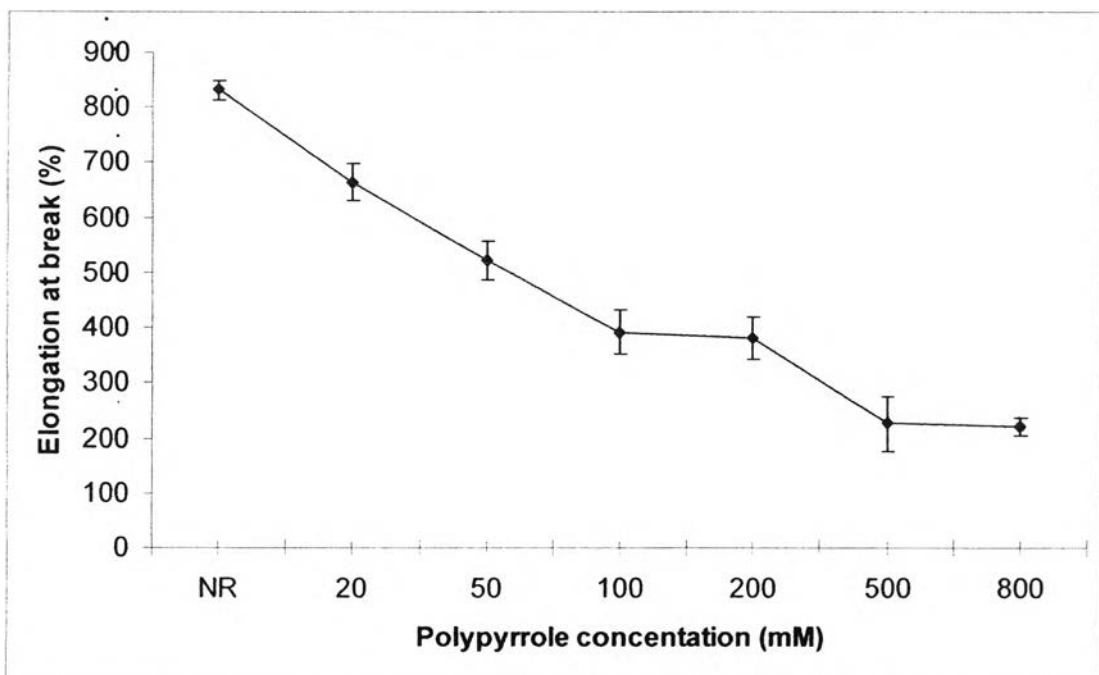


**Figure 4.45** Elongation varying the concentration of polypyrrole (Instron machine).



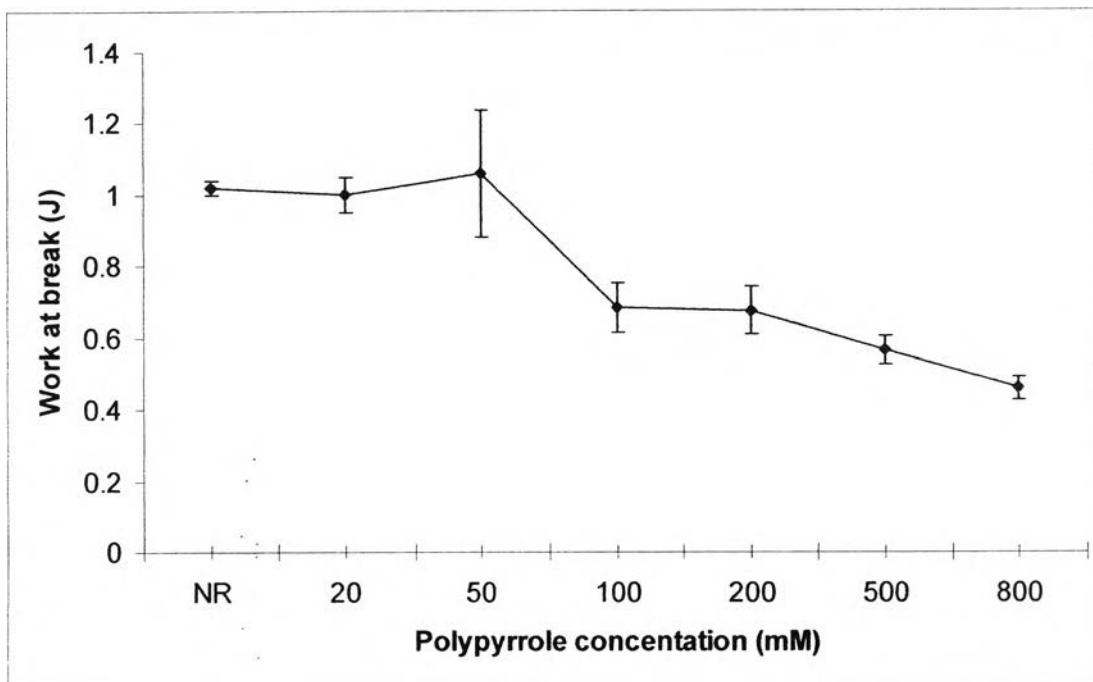


Figure 4.46 Effect of polypyrrole concentration on the energy at break.

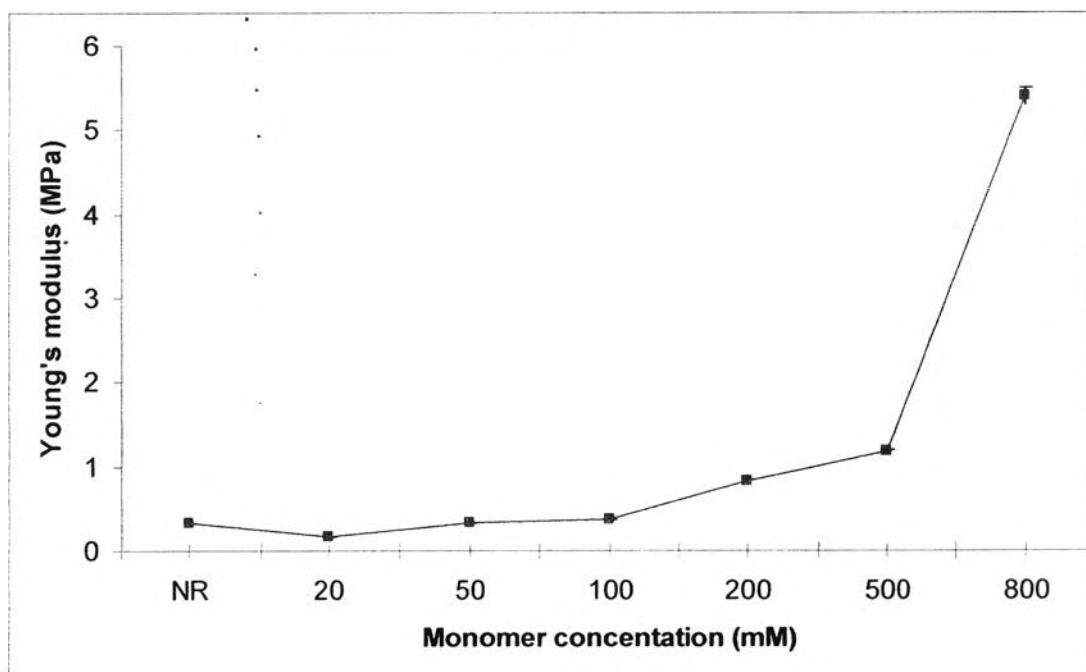


Figure 4.47 Effect of polypyrrole concentration on Young's modulus.

#### 4.4.9 Shore A and Shore D Hardness Measurement<sup>119,120,121</sup>

The shore hardness values for the samples are presented in Table 4.12. The variation of hardness of the samples is similar to that of tensile strength as shown in the Figures 4.48 and 4.49. In general, elongation of the admicellar rubber decreases whereas the hardness increases. From Table 4.12, the hardness increased from 22.46 shore A up to over the detection value of the machine, >90 shore A. The hardness was abruptly developed at about 100 mM PPy content, corresponding to the dense packing of PPy particles. The admicelled NR become hard like plastics. Thus, the hardness was measured by hardness shore D which increased from less than 10 to 25.16 shore D. The hardness of admicellar rubber corresponded to the concentration of conductive polymer which has higher hardness because of good interfacial adhesion between the matrix and the dispersed phase (S. Lopez, 2004)<sup>119</sup>. Therefore, hardness can be increased with the conductive polymer loading in the composite (Demirham, 2006)<sup>118</sup>. These are strong evidence to improve their hardness properties.

**Table 4.12** Shore hardness with concentration for admicellar rubber<sup>119,120,121</sup>

Polypyrrole concentration (mM)	Hardness (ShoreA)	Hardness (ShoreD)
NR	22.46	<10
20	30.87	<10
50	30.85	10.16
100	65.71	12.33
200	83.71	14.50
500	95.33 (>90)	17.83
800	128.33 (>90)	25.16

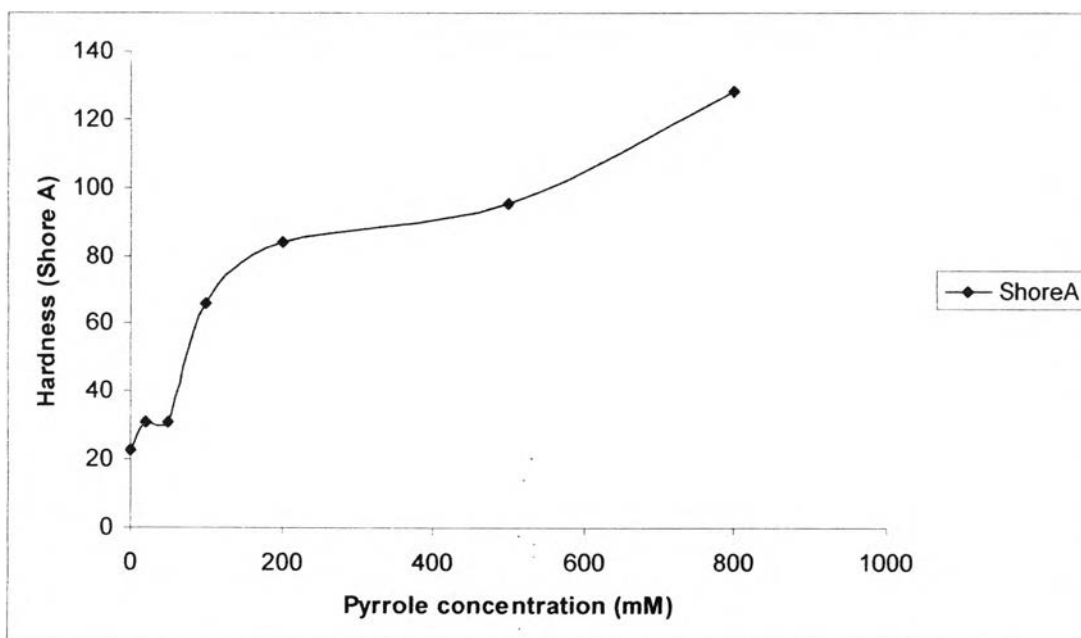


**Figure 4.48** Variation of hardness shoreA with polypyrrole concentration for admicellar rubber

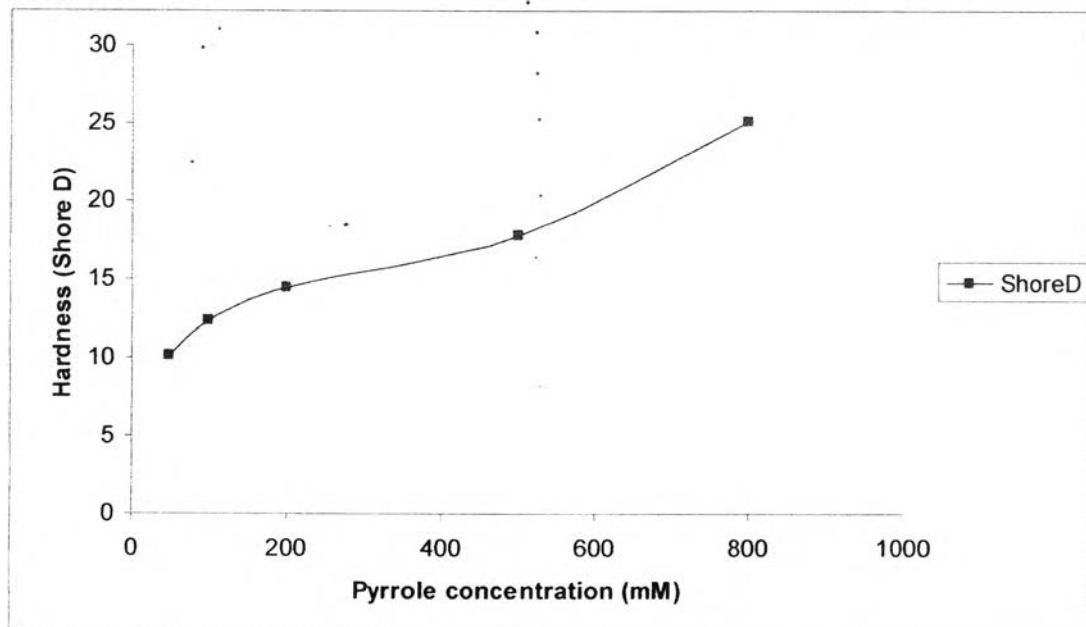


**Figure 4.49** Variation of hardness shoreD with polypyrrole concentration for admicellar rubber

#### 4.4.10 Conductivity Properties Measurement

The conductivity of admicellar rubbers were tested by using a Keithley 8009 Resistivity Test Fixture and a Keithley 6517A Electrometer/High Resistance Meter. A dc voltage of 0.1 to 15 volt was applied to the specimen placed in the Keithley 8009 test fixture. Then, the current was read and the surface and volume resistivity were determined. Figure 4.50 shows the effect of pyrrole monomer content on the electrical conductivity of admicelled PPy/NR. An electrical conductivity from  $1.49 \times 10^{-10}$  to  $3.19 \times 10^{-4}$  S/cm (20mM-800mM of PPy) could be obtained by using the electrochemical polymerization technique. In Figure 4.51, the percolation threshold of PPy in the admicelled PPy/NR products is found at volume fraction of 0.18 that raise the electrical conductivity to  $2.91 \times 10^{-6}$  S/cm, several orders from the insulator NR ( $10^{-15}$  S/cm). Then, the conductivity increases gradually with PPy content and increasing significantly at a higher concentration of PPy ( $\geq 100$  mM) in admicelled PPy/NR or volume fraction of 0.14-0.57 results in the tiny globule packing becomes denser, as a result, the rough surface coating become smooth coating surface such that the conductivity can be enhanced. The electrical conductivity as high as  $\sim 4 \times 10^{-4}$  S/cm could be finally obtained. The pyrrole promotes an increase of eleventh orders of magnitude on the conductivity of NR, ranging from  $10^{-15}$  to  $10^{-4}$  S/cm. The result is similar to that of natural rubber/polypyrrole composites, studied by Tasakorn P.[2], where adding 50% PPy can improve the conductivity as high as  $7.604 \times 10^{-3}$  S/cm. Table 4.13-4.14 are presented significantly lower volume resistivity and higher surface resistivity corresponding to physical properties, which relates to the NBR/ PANI/DBSA blends studied by Soares BG. [121]. Moreover, the results of conductivity by using this technique, electrochemical method ( $\sim 2 \times 10^{-10}$  S/cm), is lower than that of the chemical method ( $\sim 10^{-9}$  S/cm) at same amounts of PPy. These probably causes by the effects of an initiator  $\text{Fe}_2(\text{SO}_4)_3$  and salt (NaCl) which enhance the higher electrical conductivity. In addition, Bonsomsit K.[10]) found relation of surfactant and conductivity. The increasing surfactant adsorption could be increased with increasing salt, which means higher coverage and the creation of more head group sites for adsolubilization. The salt decreases the electrostatic repulsion between head-groups, which allow more adsorption and adsolubilization, which could be got higher

conductivity. However, this experiment does not focus on the relation of salts (NaCl) and  $\text{Fe}_2(\text{SO}_4)_3$ , which could be studied in the future. An electrical conductivity as high as  $\sim 4 \times 10^{-4}$  S/cm could be obtained by using this technique.

**Table 4.13** Conductivity of natural rubber sheet prepared at 25°C, 9V, at various to PPy contents

Samples (mM)	PPy : NR %	Resistivity V $\Omega \cdot \text{cm}$	$\sigma_v$ $\text{S} \cdot \text{cm}^{-1}$	Resistivity S $\Omega$	$\sigma_s$ S	Thickness (cm)
Rubber	-	1.39E+14	7.18E-15	4.07E+14	2.46E-15	0.3336
20	3.532	1.80E+09	1.49E-10	4.35E+09	2.30E-10	0.3140
50	8.408	1.67E+07	5.99E-08	2.54E+08	3.94E-09	0.2940
100	15.473	3.22E+05	3.10E-06	6.13E+05	1.63E-06	0.2925
200	26.828	2.64E+05	3.79E-06	9.68E+05	1.03E-06	0.2821
500	47.817	3.22E+04	3.11E-05	3.26E+04	3.07E-05	0.2823
800	59.4647	3.13E+03	3.19E-04	2.61E+03	3.83E-04	0.3095
PPy	100	5.91E-01	1.6921	3.52E-01	2.8373	0.000155

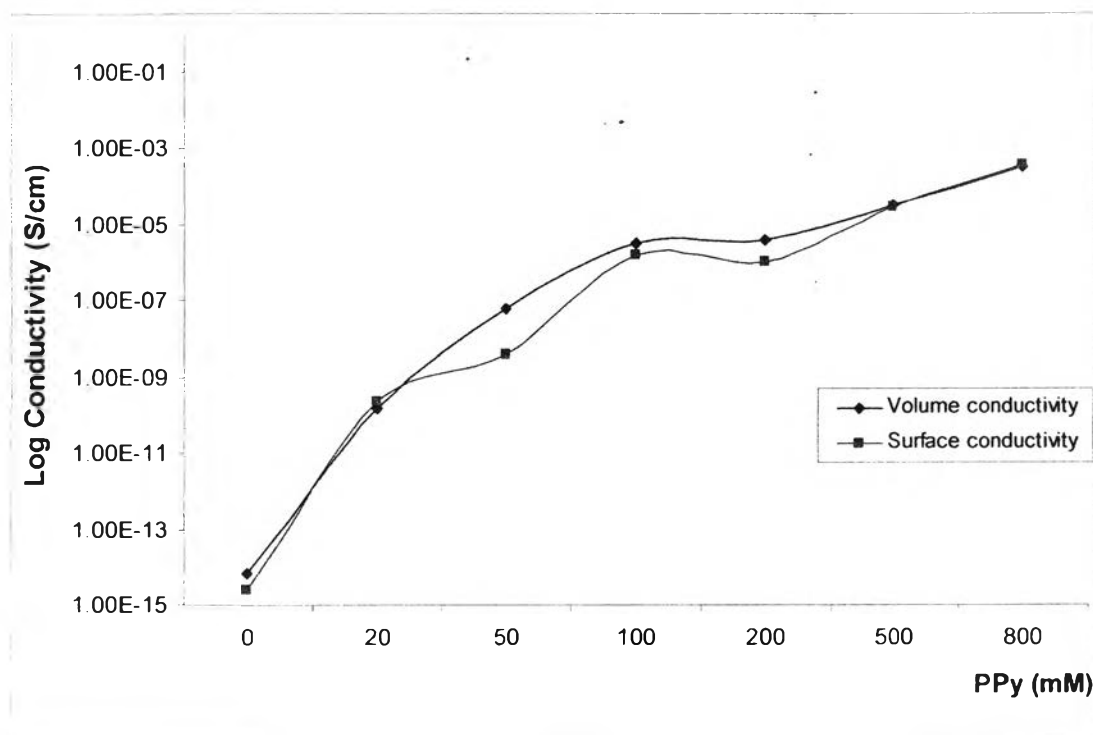


**Figure 4.50** Electrical conductivity as a function of polypyrrole content in composites with natural rubber latex (applied dc 0.1-20 volts).

**Table 4.14** Conductivity of natural rubber sheet prepared at 25°C, 9V, at various to volume fraction

Sample (mM)	$\phi_{NR} = \frac{V_{NR}}{V_{NR} + V_{PPy}}$	$\phi_{PPy} = \frac{V_{PPy}}{V_{NR} + V_{PPy}}$	$\sigma_v$ S.cm <sup>-1</sup>	$\sigma_s$ S
Rubber	1	0	7.18E-15	2.46E-15
20	0.9669	0.0331	1.49E-10	2.30E-10
50	0.9208	0.0792	5.99E-08	3.94E-09
100	0.8536	0.1464	3.10E-06	1.63E-06
200	0.7442	0.2558	3.79E-06	1.03E-06
500	0.5379	0.4621	3.11E-05	3.07E-05
800	0.4211	0.5789	3.19E-04	3.83E-04
PPy	0	1	1.6921	2.8373

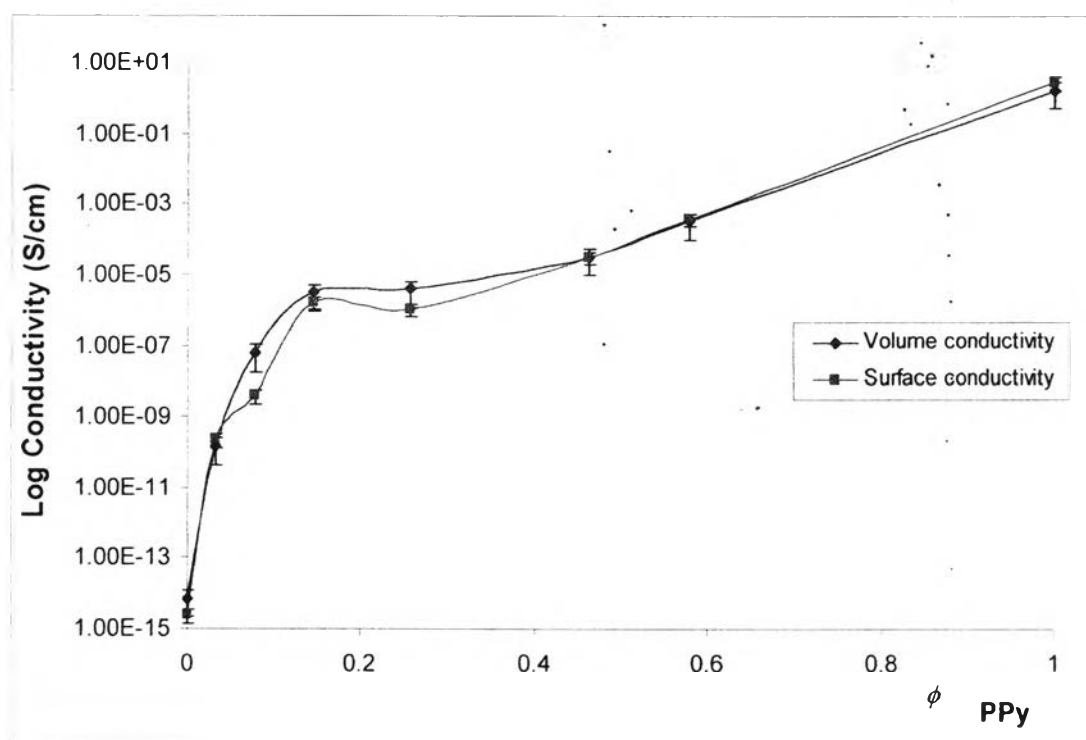


**Figure 4.51** Percolation threshold of electrical conductivity as a function of polypyrrole content in composites with natural rubber latex (applied dc 0.1-100 volts).

#### 4.5 Conclusion

The success of the admicellar polymerization of polypyrrole-coated latex particles was investigated using FTIR, SEM, TEM, and TGA. From the FTIR study, the admicelled rubbers showed the characteristic peaks of polypyrrole, which confirmed the existence of PPy after the polymerization. The TEM and SEM micrographs revealed the even coating of PPy over latex particles and they showed the core-shell structure of PPy and NR. It also confirmed the faster polymerization at higher amounts of pyrrole. This technique is efficient: % yield ~85-92%. As seen in the result of TGA, the admicelled rubbers began to lose weight at higher temperature, compared to that of NR, and they also showed the shift of major decomposition of pure PPy to higher temperature. The DTG curves also demonstrated an increase of char yields of the admicelled rubbers. As PPy content increased, the residual content also increased. This resulted in slowing down the degradation of admicelled rubber at 260 to 375°C. These indicated that the admicelled rubbers were more thermostable than natural rubber. This suggested that admicellar polymerization via the electrochemical method was a unique method to prepare a good miscible core-shell structure of PPy-NR. The mechanical properties from tensile testing showed the decrease of work to break of the admicelled rubbers. This indicated the higher stiffness of the admicelled rubbers compared to natural rubber. Since the PPy behaved like a hard and brittle material, the stiffness of the materials increased as PPy content increased. The effect of conductivity revealed that the addition of polypyrrole at the same condition, 9V, 25°C, pH ~3, allowed more adsorption and adsolubilization, leading to an homogeneous coating of PPy over the rubber surface. However, too much voltage is not good to stabilized leading to the contamination in admicellar rubber due to copper corrosion. The conductivity increased from  $\sigma = 10^{-15}$  S/cm at 0%wt of PPy to  $\sigma = 10^{-4}$  S/cm at 51%wt PPy (800mM). As PPy content increased, the conductivity was also increased because the coating of PPy was more perfect at higher concentration, as supported by TEM and SEM micrographs and the result of TGA. The higher number of polymer chains was obtained when content was high to abstract electron from pyrrole and enhance free radical polymerization, resulting in higher conductivity and greater in their density.

#### **4.6 Acknowledgements**

The authors would like to acknowledge the Rachadapisek Sompoch Endevelopment (RU), Chulalongkorn University, for their financial support for this project. The author would like to acknowledge the Petroleum and Petrochemical College; the National Excellence Center for Petroleum, Petrochemicals, and Advanced Materials, Thailand; the National Research Council of Thailand.